Nutrient loads from agricultural catchments in response to extreme wet or dry conditions

How will N and P loads change with climate change?

Inger Hellstrand

Master's thesis in soil science • 30 credits
Swedish University of Agricultural Sciences, SLU
Faculty of Natural Resources and Agricultural Sciences
Department of Soil and Environment
Agronom mark och växt
Examensarbeten / Institutionen för mark & miljö, SLU
Partnumber: 2026:08
Uppsala, 2026

Nutrient loads from agricultural catchments in response to extreme wet or dry conditions

Näringstransporter från jordbruksområden vid extremväderförhållanden

Inger Hellstrand

Supervisor:	**Sara Sandström, SLU, Department of Soil and Environment**
Assistant supervisor:	Jennie Barron, SLU, Department of Soil and Environment
Examiner:	Helena Aronsson, SLU, Department of Soil and Environment

Credits:	30 credits
Level:	A2E (advanced)
Course title:	Independent project in Soil Science - Agriculture
Course code:	EX1053
Programme/education:	Agronom mark och växt
Course coordinating dept:	Department of Soil and Environment
Place of publication:	Uppsala
Year of publication:	2026
Number in series:	2026:08
Series title:	Examensarbeten / Institutionen för mark och miljö, SLU
Cover picture:	Lisbet Norberg

Keywords:	total nitrogen, total phosphorus, agricultural catchments, extreme weather events, SPEI, long-term monitoring, Sweden

Swedish University of Agricultural Sciences
Faculty of Natural Resources and Agricultural Sciences
Department of Soil and Environment

Abstract

Climate change is predicted to lead to more frequent and intense extreme weather events, which poses a risk of increased nutrient leaching from agricultural land and as a consequence, worsened eutrophication in aquatic ecosystems. The aim of this thesis was to investigate how long-term trends in nitrogen and phosphorus export are influenced by extreme wet or dry conditions. The research question was: How do extreme wet and extreme dry periods affect total nitrogen (TN) and total phosphorus (TP) loads in agricultural catchments in southern Sweden?

To answer this, 30 years of environmental monitoring data from three small agricultural catchments (I28, M42, and N34) were analysed. The Standardised Precipitation-Evapotranspiration Index (SPEI) was applied at multiple timescales to identify periods of hydrological stress, which was combined with Generalised Additive Models (GAM) for trend analysis and event-based high-flow separation.

The results showed that wet agrohydrological years were associated with substantially higher nutrient export and more frequent high-flow events than dry years. In catchment N34, approximately 19% of the days during 1998–2002 had SPEI-3 values > 1.5, yet these periods accounted for around 70% of annual TN export. Similar patterns were observed for TP export during prolonged wet periods. TN export was primarily associated with sustained hydrological transport and subsurface flow pathways, whereas TP export showed a more episodic response linked to runoff events and first-flush processes.

The study further demonstrated that SPEI provided important hydrological context beyond runoff-based event identification alone. SPEI-1 showed the most consistent and statistically significant relationships with nutrient export across all three catchments and both nutrients, indicating the importance of antecedent moisture conditions and short-term hydrological variability. During dry periods, reduced hydrological connectivity generally lowered annual nutrient export, although prolonged drought conditions also appeared to increase the risk of elevated nutrient mobilisation during subsequent rewetting events.

In conclusion, current field-scale mitigation measures may be insufficient during extreme weather events, as they are not designed for the massive water volumes generated. To mitigate extreme nutrient export in a future climate, mitigation strategies must increasingly shift towards landscape-level measures focused on water retention.

Keywords: total nitrogen, total phosphorus, agricultural catchments, extreme weather events, SPEI, long-term monitoring, Sweden

Sammanfattning

Klimatförändringarna förväntas leda till fler och mer intensiva extrema väderhändelser, vilket innebär en risk för ökat näringsläckage från jordbruksmark och till följd ökad övergödning i akvatiska ekosystem. Syftet med detta arbete var att undersöka hur långsiktiga trender i kväve- och fosfortransport påverkas av extrema blöta och torra perioder. Forskningsfrågan är: Hur påverkar extrema blöta och extrema torra perioder totalkväve- (TN) och totalfosfor- (TP) belastning i jordbruksdominerade avrinningsområden i södra Sverige?

För att besvara detta analyserades 30 års miljöövervakningsdata från tre små jordbruksdominerade avrinningsområden (I28, M42 och N34). Standardised Precipitation-Evapotranspiration Index (SPEI) användes på flera tidsskalor för att identifiera perioder av hydrologisk stress, vilket kombinerades med Generalised Additive Models (GAM) för trendanalys samt händelsebaserad separation av högflöden.

Resultaten visade att blöta agrohydrologiska år var associerade med avsevärt högre näringstransport och en ökad frekvens av högflödeshändelser jämfört med torra år. I avrinningsområde N34 hade cirka 19 % av dagarna under perioden 1998–2002 SPEI-3-värden > 1,5, men dessa perioder stod för omkring 70 % av den årliga TN-transporten. Liknande mönster observerades för TP-transport under långvarigt blöta perioder. TN-transport var främst kopplad till kontinuerligt och ihållande läckage via flödesvägar under markytan, medan TP visade en mer episodisk respons kopplad till ytavrinning och första flödesevent (first-flush event).

Studien visade vidare att SPEI gav viktig hydrologisk kontext utöver enbart flödesbaserad händelseidentifiering. SPEI-1 uppvisade de mest konsekventa och statistiskt signifikanta sambanden med näringstransport i samtliga avrinningsområden och för båda näringsämnena, vilket indikerar att kortsiktiga skiften i markfuktighet är avgörande för mobilisering av näringsämnen. Under torra perioder minskade generellt näringstransporten till följd av minskad hydrologisk konduktivitet, men långvarig torka kunde samtidigt öka risken för förhöjd mobilisering vid efterföljande avrinning.

Sammanfattningsvis tyder resultaten på att nuvarande åtgärder på fältnivå kan vara otillräckliga under extrema väderhändelser, eftersom de inte är dimensionerade för de stora vattenvolymer som genereras. För att minska extrema näringsförluster i ett framtida klimat behöver åtgärder i högre grad vara på landskapsnivå med fokus på vattenhållande och fördröjande funktioner.

Table of contents

List of figures

List of tables

Abbreviations

Abbreviation	Description
PP	particulate phosphorus
SPEI	Standardised Precipitation–Evapotranspiration Index
SS	suspended solids
TN	total nitrogen
TP	total phosphorus

1. Introduction

1.1 Climate change impact

Climate change is predicted to cause losses in crop production, due to heat and dry conditions, and extreme weather is expected to be increase in frequency (Intergovernmental Panel On Climate Change (IPCC) 2023). Extreme weather events with floods and droughts have become more likely and/or more severe due to climate change (FAO 2025). Agricultural drought and ecological drought have increased on all continents due to an increase in evapotranspiration (Muhammad et al. 2023). Agricultural drought is defined as a period when there is too little water in the soil for a crop to grow (Wilhite & Glantz 1985). Ecological drought is a disturbance that pushes natural and human systems beyond their capacity to adapt, triggering significant socioecological feedbacks (Crausbay et al. 2017). To maintain food security in the world, understanding the impact of climate-related stressors (e.g. droughts, floods, and heat waves), on agriculture is crucial (IPCC 2023). The hydrological climate in the Nordic regions is changing and is expected to do so in the future as well (De Wit et al. 2020). Over the past six decades, Sweden has undergone hydrological changes, characterised by a temperature increase of 2.2 °C and a 20% increase in total annual precipitation in the period 1961 to 2020 (Teutschbein et al. 2022). Despite a general national trend towards wetter conditions, southern Sweden remains more vulnerable to extreme events, where streamflow droughts (when streamflows levels are unusually low) are often more frequent and severe compared to northern regions (Teutschbein et al. 2022).

Runoff from agriculture containing agrochemicals such as nutrients and pesticides degrades water quality in multiple ways, for example increasing eutrophication and impacts the loss of marine life (European Environment Agency (EEA) 2025). EEA advocates for an urgent need of change for Europe′s agricultural sector to adapt to extreme weather events to guarantee the EU′s long-term food security. EEA (2025) claims extreme weather is a key challenge for Europe’s agricultural sector. For example, even Europe's highly developed and technologically advanced cereal production systems may face average yield reductions of approximately 20% as a result of extreme weather events. In a changing climate, mitigation measures at the catchment scale (e.g., buffer zones and artificial wetlands) to reduce nutrient-runoff may be insufficient to protect water quality (De Wit et al. 2020). However, recent research has found that even though the flow would be lower during summer the annual nitrogen (N) removal would be the same since the winter removal would increase. The authors emphasise on the importance of wetland design and vegetation cover for effective N removal in wetlands created in agricultural landscapes (Nilsson et al. 2023).

Predicting nutrient mobilisation in agricultural landscapes is inherently complex, primarily due to significant spatial and temporal variability. Research across diverse catchment characteristics indicates that changes in pollutant loading generally correlate with projected shifts in precipitation and runoff (Coffey et al., 2019). In particular, the increasing frequency of heavy precipitation events is expected to drive more episodic pollutant loading to water bodies, where nutrients accumulated during dry periods are rapidly mobilised during high-flow events (Coffey et al. 2019; IPCC 2023).

Diffuse nutrient fluxes in agricultural systems are shaped by the hydro-climatic variability and landscape characteristics (De Wit et al. 2020). Factors such as soil properties, crop cycles, and land-use management interact over time to determine the overall magnitude of nutrient export from the catchment. As noted by De Wit et al. (2020), understanding these spatial and temporal drivers is essential for predicting the environmental response to changing management and climate.

1.2 Hydrological extremes

Diffuse legacy sources, e.g. nutrients originating from historical land-use activities and released gradually from environmental stores across the landscape, are the dominant contributors to the currently observed stream concentrations and loads of both N and phosphorus (P) in Sweden (Han et al. 2024). National statistics from 2022 indicate a tightly managed nutrient balance, with a surplus of 29 kg N per hectare and a slight deficit of -1 kg P per hectare at a national scale (Statistiska centralbyrån (SCB) 2024). Of the N surplus, leaching losses accounted for 14 kg/ha, while only 2 kg/ha contributed to soil build-up or denitrification. This suggests that current fertilisation practices do not lead to significant accumulation, especially for P. However previous excessive fertilizer and manure use results in the accumulation of nutrients in soils, a legacy, which under the right environment can be transported to freshwater systems through runoff and leaching (Molina-Navarro et al. 2018).

Droughts and heatwaves tend to decrease concentrations where the main source of nutrients is diffuse e.g. agricultural land, due to decreasing runoff loads and increasing retention (Mosley 2015). During floods however, the concentration of nutrients in particulate form e.g. P, tend to increase due to increasing erosion and remobilisation of nutrient sources (Bieroza & Heathwaite 2015).

After a long dry period, seasonal first-flush can contribute to a significant P load in runoff and receiving waters (Gu et al. 2018). First-flush phenomena are when the initial storms of the season have higher nutrient loads than the storms later in the

season (Yang et al. 2021). The load of the first-flush varies depending on the type of nutrients and their characteristics (Yang et al. 2021).

According to Williams et al. (2015), 2% of the highest runoff flows, transported more than 50% of the annual dissolved reactive P (DRP) in their study in Ohio, USA and Ontario, Canada. During the same period N on the other hand transported only 26% of annual NO_3-N load, which highlights the differences between DRP and NO_3-N transport processes. Similar event-driven patterns have been quantified in Sweden, where high-frequency monitoring has revealed the complexity of nutrient mobilisation during storms (Bieroza et al. 2014; Lannergård 2021). Furthermore, extreme total P (TP) concentration peaks, as well as nitrate dilution episodes, occurs during storm events with high precipitation (Dupas et al. 2024). The peaks intensified after either a period of drought or lower flows (Dupas et al. 2024). High runoff events are responsible for the majority of P loss in agricultural drained discharge (Dialameh & Ghane 2023).

1.3 Agricultural catchments

Concentrations of total N (TN) and TP are largely driven by land-use, along with having a climate gradient, where the highest nutrient concentrations were associated with warmer regions (De Wit et al. 2020). Hence, climate and land-use are deeply related which implies that identification of separate impacts of these two factors is challenging (De Wit et al. 2020; Petersen et al. 2021). When comparing nutrient losses from different catchments it is important that they have similar land-use types depending on the aim of the comparison.

Soil texture and structure play a critical role in nutrient export pathways. Permeable soils, e.g. sandy soils, generally promote nitrate leaching due to low adsorption capacity. Soluble nitrate-N is transported through the soil profile either to the drainage system or directly to the groundwater (Kyllmar et al. 2023). In fine-textured clay soils nutrients tend to retain but could be rapidly transported via macropores, leading to episodic P losses during high-flow events (de Jonge et al. 2004). Riparian zones are important in a watershed since they are effective at removing nutrients. A significant proportion of agricultural land in Sweden relies on drainage systems; according to national statistics, approximately 60% (1.53 million ha) of arable land is considered satisfactorily drained, of which 43% (1.06 million ha) is system tile-drained (Jordbruksverket 2023). This extensive drainage network modifies the riparian function in the watershed by bypassing natural filter strips and creating direct pathways for nutrient transport (Decker et al. 2024).

Small headwater catchments with no point sources of nutrients offer an ideal basis to assess both land-use and climate impacts on nutrient export, since nutrient retention is not happening in the same degree compared to larger streams (Weigelhofer et al. 2018). However, interpretation of nutrient dynamics in such systems requires long-term monitoring. Short-term datasets (<4 years) often fail to capture the high inter-annual variability in nutrient export driven by hydrological fluctuations, and may therefore lead to inconclusive assessments of mitigation efficiency (Liu et al. 2017). This is particularly relevant for P, where event-driven transport can cause large year-to-year variability in total loads (Sharpley et al. 1999).

1.4 Nitrogen

Already over 20 years ago Arheimer et al. (2005) suggested that in a future climate there will be an increased annual load of N from land to sea (22%) due to an expected increase of high winter flow. The annual costs of water pollution from N and P (predominantly from agriculture) in the EU is estimated to be over EUR 22 billion yearly (European Commission et al. 2021).

Diffuse N losses from intensive agricultural production, together with P losses, leads to eutrophication in aquatic ecosystems (Sobota et al. 2015). N that is not washed out from the soil could stay in the soil and groundwater, creating a N pool legacy. Hence N could leach out from the soil even if the input of N ceased, up to decades afterwards (Van Meter et al. 2016; Metaxoglou & Smith 2025). Having the knowledge about these storages in the soil profile and groundwater is crucial since it is important in creating realistic timelines regarding N mitigation measures.

The mobility of N is highly dependent on its chemical form (Eriksson 2011). Ammonium (NH_4^+) is generally retained in the soil because it binds to the negative surfaces of soil particles or becomes fixed within clay minerals. However, NH_4^+ is typically transformed quickly into nitrate (NO^{3-}) through nitrification, a highly effective process in aerated agricultural soils as long as temperatures remain above freezing. In contrast, nitrate is an anion and does not bind to soil complexes, making it highly mobile. The risk of leaching is therefore closely linked to the concentration of NO^{3-} in soil solution, whether it originates from fertilizer application or the mineralisation of organic N (Eriksson 2011). Nitrate, typically constitutes the dominant fraction of TN export in agricultural catchments at annual scales and is mainly transported via subsurface and groundwater flow paths, whereas particulate N becomes more important during storm events when surface runoff and erosion are activated (Jiang et al. 2010).

Soil texture significantly influences N transport pathways (Eriksson 2011). Generally, N leaching is higher from soils with less than 25% clay, as water saturation and transport are more effective in these coarser textures. Furthermore, clay-rich soils often facilitate higher rates of denitrification, where nitrate is lost to the atmosphere as gas rather than leaching into the groundwater. While a rough mean estimate for N leaching from agricultural soils is approximately 2000 kg/km^2/year, this varies greatly depending on crop, fertilisation strategies, and soil management (Eriksson 2011).

The mineralisation of N and nitrification happens during autumn in temperate climates and is the most important reason for leaching of N (Eriksson 2011). Therefore, ploughing during early autumn is not recommended. Applying N in excess of crop requirements significantly increases the leaching risk, particularly during heavy precipitation events where unused N can be rapidly washed away (Eriksson 2011). The technical problem with dispersing fertilisers a few times per year creates the risk of the not used N to be washed away by a rainstorm, which could be less of a problem in the future with technical improvements regarding fertiliser dispersion (Metaxoglou & Smith 2025).

1.5 Phosphorus

P losses degrade water quality by stimulating algal growth and eutrophication, resulting in substantial societal costs associated with water treatment, ecosystem restoration, and loss of ecosystem services, estimated at approximately $1 billion annually in Europe (Wurtsbaugh et al. 2019).

Transport of particulate P (PP) is linked to transport of suspended solids (SS) in small agricultural streams, where a high clay content leads to higher SS losses (Sandström et al. 2020). In the soil, P is highly reactive and tends to "stick" to soil surfaces, retained through sorption reactions to aluminium (Al) and iron (Fe) oxides or by precipitating as calcium or magnesium phosphates (van Doorn et al. 2024). The degree of saturation of P can be approximated by agronomic soil test P (STP) e.g. P-AL (Djodjic et al. 2004) or Olsen-P (Johnston et al. 2014). P losses are not only controlled by soil P content, but also by erosion processes governed by soil structure and texture (Sandström et al. 2020), as well as P sorption capacity.

P transport by surface runoff can be both infiltration-excess and saturation-excess mechanisms. Surface runoff from infiltration-excess is often the result of high-intensity storms or precipitation onto surfaces exposed to e.g. excessive vehicle or animal traffic that could create pores in the soil surface. This kind of runoff is fast and highly erosive, resulting in more PP losses than under saturated conditions

where runoff occurs because the soil is fully saturated (Kleinman et al. 2006). The probability of infiltration-excess runoff and PP loss is increasing with climate change, in response to drought, floods and the greater likelihood of storms (Ockenden et al. 2017).

Consequently, P export from agricultural catchments is highly episodic and strongly event-driven, governed by the interaction between soil P availability, erosion processes, and hydrological connectivity. PP transport is particularly associated with storm events, leading to disproportionate downstream loads during short periods of high discharge (Sharpley et al. 1999).

1.6 Objectives

The aim of this thesis is to investigate how long-term trends in N and P export are influenced by extreme wet or dry conditions in three small agricultural catchments in Sweden over a three-decade period. At the moment, there is limited knowledge on P and N transport related to extreme weather events in Sweden, and this knowledge gap is something that this master project will fill. This research field is very important, regarding climate change impact on future climate and will hopefully bring useful information about how to plan agricultural management and policy regarding lowering nutrient loads as well as eutrophication.

The main research question for this project is:

- How do extreme wet and extreme dry periods affect TN and TP loads in agricultural catchments in southern Sweden?

2. Material and methods

The following study was conducted in several steps.

1. Selection of catchments.
2. Long-term hydrological calculation using Standardised Precipitation-Evapotranspiration Index (SPEI).
3. Comparison of annual TN and TP loads across wet, dry, and normal years.
4. Event-scale analysis of selected extreme years.

2.1 Catchments

In Sweden, N and P loads in eight agricultural catchments (470–3300 ha) have been intensively monitored for >30 years through the Agricultural Catchments Monitoring Program, coordinated by Swedish University of Agricultural Sciences (SLU) and funded by the Swedish Environmental Protection Agency (Kyllmar et al. 2014). Out of those eight, this study has been narrowed down to three specific catchments: I28, N34, and M42 (Figure 1). The data used in this study were retrieved from the national monitoring database (SLU 2026).

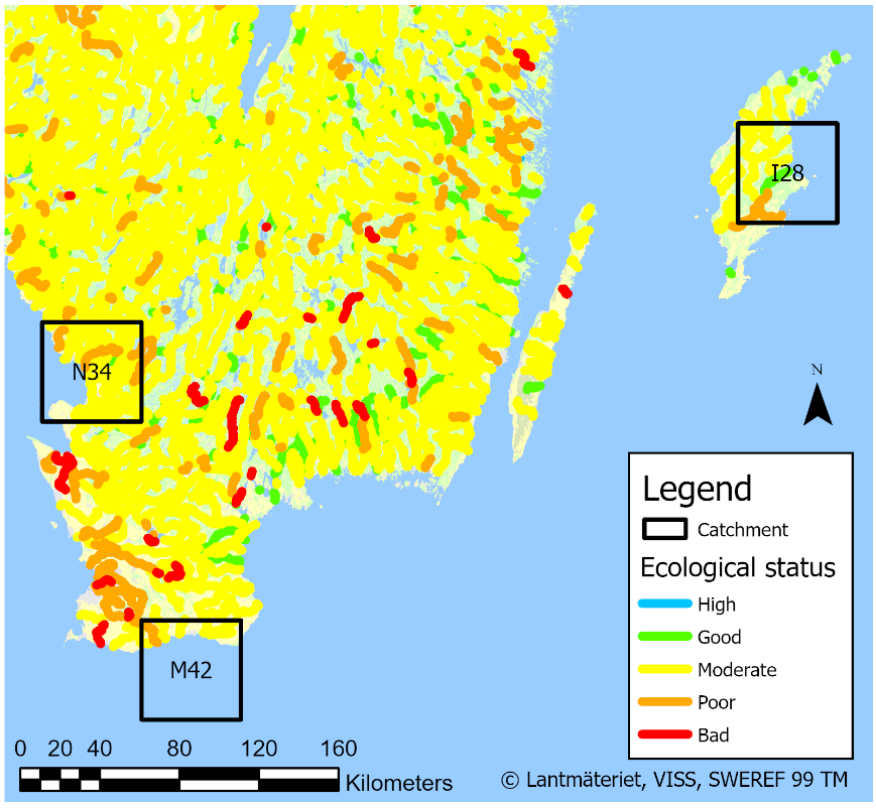

Figure 1. Ecological status (Ecological quality ratio, EQR) in watercourses over southern Sweden (Vattenmyndigheterna 2025; Lantmäteriet 2026). High 0.7≤EQR, Good 0.5≤EQR< 0.7, Moderate 0,3≤EQR≤0.5, Poor 0.2≤EQR≤0.3, Bad EQR<0.2 (Svensson 2022). Since the catchments exact placement is classified, the location is somewhere in this 50 X 50km square.

The three catchments were selected to represent a gradient of hydrological regimes and regional climate characteristics in southern Sweden, while maintaining similarities in catchment size (470–1393 ha) and land-use intensity (>75% arable land and >90% drained land). These catchments are all situated in an area with waterbodies with an overall ecological status classified as moderate (cycle 2016-2021) by the Water Information System Sweden (Figure 1) (Vattenmyndigheterna 2025). See Appendix 2 for calculation of Ecological status. In Sweden, nutrient status is classified into five categories (High, Good, Moderate, Poor, Bad) based on thresholds defined by the Swedish Agency for Marine and Water Management in regulation HVMFS 2019:25 (Havs- och vattenmyndigheten 2019), which implements the EU Water Framework Directive (WFD) (European Parliament and Council 2000). These thresholds are determined using type-specific reference values and Ecological Quality Ratios (EQR), comparing current nutrient concentrations to estimated natural conditions for different water bodies.

Table 1. Characteristics of the studied catchments I28, M42, and N34, including location, total, arable and drained area, soil type, normal precipitation, main crops, TN and TP input, P-AL class, and study period (Linefur et al. 2024).

Catchment ID	Location	Climate Zone (Köppen)[1]	Total area (km^2)	Arable land (%)	Drained arable land (%)	Soil type (FAO classification)	Average annual precipitation ±STD (mm)[2]	Main Crops (2015-2023)	TN Input (kg N/ha)	TP input (kg P/ha)	P-AL Class[3]	Study period
I28	Gotland, Baltic Sea	Humid Continental (Dfb)	4.79	78	99	Loam	671.7 ± 129.3	Winter wheat, spring barley, ley, winter rape, legume, potato	160-170	23	IVa	1989 – 2024
M42	Southern part of Skåne, Sweden	Humid Continental (Dfb)	8.24	91	100	Loam	555.4 ± 118.5	Winter wheat, sugar beets, spring barley, winter rape, ley, legumes	140–150	10-20	IVb	1992 – 2024
N34	Halland plains, Laholm Bay drainage area	Humid Continental (Dfb)	13.93	85	93	Sandy loam	740.4 ± 185.1	Winter wheat, spring barley, ley, winter rape, potato	150	20	IVb	1996-2024

1. (Peel et al. 2007) *2.Values represent averages ± STD calculated from the study period (1989–2025). 3.(Sandström et al. 2020)*

2.2 Sampling method

Manual grab sampling has taken place since the 90s for all catchments, in 2004 the sampling method changed to flow-proportional sampling for M42 and N34, I28 changed in 2005. During flow-proportional sampling, a logger calculates the current flow rate and once a specific volume of water has passed the monitoring point a sub-sample of approximately 15 ml is drawn using a peristaltic pump. These sub-samples are collected in a glass bottle, where the total volume varies following the magnitude of the runoff. The pooled sample is typically collected once every two weeks, at which point a representative sample for analysis is taken and the bottle is emptied. During low-flow periods, the system switches to time-integrated sampling (two samples per day) to ensure sufficient sample volume for analysis. Water samples have been analysed at the SLU, Department of Aquatic Sciences and Assessment, which is an accredited laboratory following ISO SS-EN ISO 6878:2005 for TP and ISO SS-EN ISO 20236:2021 since 2014. See Appendix 7: Table A4 for full history.

2.3 Calculation of water discharge and nutrient loads

Area-specific transport (kg/km^2) was calculated by dividing the total transport (kg) by the total area of the catchment (km^2). Area-specific runoff (mm) was calculated from daily mean discharge values (l/s). All calculations of annual water discharge and nutrient loads are based on the agrohydrological year, which runs from July 1st to June 30th. Hereafter, this is referred to simply as "year" (e.g., 1998/1999), unless otherwise specified. Agrohydrological years are used since it aligns with previous studies conducted within the Agricultural Catchment Monitoring Program (Linefur et al. 2024; SLU 2025) thereby ensuring comparison with earlier findings. This division is considered appropriate as it integrates both hydrological and agronomic processes. From a hydrological perspective, the division is placed during a period of relatively low subsurface discharge, reducing the risk of dividing a continuous runoff event between two years. From an agronomic perspective, the agricultural cycle typically coincides with harvest in late summer, followed by autumn tillage or sowing of winter crops, marking the beginning of a new cropping season.

Daily concentrations for flow-proportional samples, representing the water that passed the monitoring station during a two-week period, were calculated by extrapolating the analysed values back to the day following the previous sampling event. The composite sample is thus considered representative for the entire period between two sampling occasions. Daily transports were thereafter calculated using the same method as for grab samples. To calculate annual loads, all daily loads for that year were summed.

2.4 Meteorological data

Meteorological data were primarily sourced from the Swedish Meteorological and Hydrological Institute (SMHI) national station network (SMHI 2026), supplemented by measurements from the Lantmet network operated by SLU (Lantmet 2026). SMHI is the standardised official infrastructure for meteorological monitoring in Sweden, ensuring high data quality and technical calibration.

1. Precipitation: To ensure methodological consistency and direct comparability with national monitoring reports (Linefur et al. 2024), precipitation stations were selected to align with those used in the National Monitoring Programme for Agricultural Catchments (*Typområden på jordbruksmark*).
2. Temperature and wind: Data were retrieved from official SMHI reference stations located within a 30 km radius of the study catchments to accurately reflect local climatic conditions.
3. Relative humidity and solar radiation: Due to the lower density of monitoring sites for these parameters, the geographical range was extended to include the nearest representative regional stations within the SMHI or Lantmet networks.

2.4.1 Gap filling and interpolation

To maintain a continuous time series, missing data points were handled based on the duration of the gap:

1. For general gaps in the dataset, data was filled in from the next prioritised station in the hierarchy.
2. For short-term gaps of less than three consecutive days linear interpolation was used in R performed by the author.

2.5 Water balance index

Standardised Precipitation–Evapotranspiration Index (SPEI) is broadly used for meteorological drought analysis (Vicente-Serrano et al. 2010; World Meteorological Organization & Global Water Partnership 2016). SPEI compares current moisture conditions to what is normally expected for that specific location and season. Values around zero indicate normal conditions, positive values indicate wetter-than-normal conditions, and negative values indicate drier-than-normal conditions. This index is one of the most suitable indices for capturing the impacts of agricultural drought. The Standardised Precipitation Index (SPI) is common, although SPEI is better suited for investigating climate change trends since it integrates potential evapotranspiration (PET), which reflects atmospheric

evaporative demand (Beguería et al. 2010; Vicente-Serrano et al. 2010; 2012). Evapotranspiration plays a key role in drought severity, and inclusion of PET is therefore recommended in drought index calculations. The Penman–Monteith equation was selected over temperature-based approaches to ensure a more physically based estimation of PET (Allen 1998; Vicente-Serrano et al. 2012). In the Swedish landscape, characterised by significant seasonal variations in solar radiation, temperature and wind patterns, including these parameters is essential for accurately capturing the water balance. An advantage of SPEI is that it allows comparisons between different years and regions compared to other indices (Sjulgård et al. 2023). Assessing dry periods in Sweden based on both precipitation and evapotranspiration leads to a greater number of periods identified compared to using SPI, since it can be a drought even though it is a high rain event if it simultaneously is a high temperature or windspeed (Canedo Rosso et al. 2025).

In this study, SPEI was calculated at four different timescales, 1, 3, 6, and 12 months (SPEI-1, SPEI-3, SPEI-6, and SPEI-12). Different timescales capture different hydrological dynamics, SPEI-1 captures short-term changes in near-surface soil moisture, SPEI-3 reflects seasonal moisture conditions, while SPEI-12 reflects hydrological stress. The calculations were performed using the package *SPEI* (Beguería & Vicente-Serrano 2023) in R (R Core Team 2024). The four scales were conducted to see the differences over the years using different time reference periods. For detailed event-scale analysis within specific agrohydrological years, the 3-month timescale (SPEI-3) was selected, as it effectively captures the seasonal shifts in moisture conditions that drive nutrient mobilisation. The 12-month timescale (SPEI-12) was used to identify overall long-term wet and dry periods. Periods where SPEI-12 was ≤ -1.5 or ≥ 1.5 for at least two consecutive years were identified and analysed in more detail.

The calculation of SPEI required a comprehensive set of daily meteorological parameters, including Precipitation (Pre), Temperature maximum and minimum (T), Wind speed at 2 meters height (u_2), Relative Humidity and Solar Radiation (R_n). These data were retrieved from the SMHI Open Data services (SMHI, 2026) and from the Lantmet station network, managed by SLU (Lantmet 2026). All data were obtained for the period 1989–2025 for the monitoring stations relevant to catchments M42, N34, and I28. PET was calculated using the FAO Penman–Monteith equation (Eq.1), thereby representing reference evapotranspiration (ET_0). Subsequently, the climatic water balance (D) was calculated using equation (Eq. 2).

$$(1)\ ET_0 = \left(0.408\Delta(R_n - G) + \gamma \frac{900}{T+273} u_2 (e_s - e_a)\right) / \left(\Delta + \gamma(1 + 0.34u_2)\right)$$

$$(2)\ \text{Pre} - ET_0 = \text{D}$$

See Appendix 1 for full description of Penman-Monteith.

2.6 Data visualisation and statistical graphics

All statistical analysis and visualisation was done in R (4.2.2) (R Core Team 2024).

2.6.1 Annual and temporal distributions

Annual nutrient loads were calculated by summing monthly areal transport values within each agrohydrological year (July–June). When both manual and flow-proportional sampling were available for the same month, the mean monthly transport was used to avoid double counting. Monthly areal transport data were only available from 2006 in M42, resulting in a shorter time series for annual load calculations compared to I28 and N34.

Boxplots

The results are displayed in boxplots to highlight the difference in annual loads of TN and TP between the catchments, as well as showing the range for every catchment. Every point indicates a specific year, colour coded based on the hydrological status from the SPEI-12 value. Dry years (red) indicate average SPEI-12 < -1, normal years (grey) $-1 \leq$ average SPEI-12 ≤ 1, and wet years (blue) average SPEI-12 > 1.

Line diagram

The results are additionally displayed in line diagrams to highlight changes in annual loads of TN and TP between years during the study period. In addition, this enables the comparison between different catchments in annual loads.

2.6.2 Long-term trend analysis

GAM

Non-linear trends in concentrations and loads were analysed using Generalised Additive Models (GAM) using the package *screenmodeling* (von Brömssen et al. 2020) in R (R Core Team 2024). This approach is specifically designed for the analysis of large-scale environmental time series with irregular sampling frequency and temporal dependence and is commonly used in Swedish monitoring studies (e.g. Kyllmar et al. 2023). The model includes a smooth function of time to capture significant non-linear trends. The significant trends were colour coded accordingly: decreasing (blue), increasing (red), and no significant trend (yellow), based on the first derivative of the smooth term with a 95% confidence interval and trends were considered statistically significant at $p < 0.05$.

2.6.3 Statistical correlation analysis

Spearman

To evaluate the relationship between hydroclimatic conditions and nutrient export, Spearman's rank correlation analysis (ρ) was applied. This non-parametric method was chosen due to the non-normal distribution of hydrological event data and the potential presence of non-linear relationships between variables. Correlations were calculated separately for each of the three study catchments (M42, N34, and I28) and for both TN and TP. All analyses were performed using R (R Core Team 2024) and base functions. The analysis examined the relationship between the proportional contribution of individual hydrological events to annual total TN and TP loads (%) and the Standardised Precipitation-Evapotranspiration Index (SPEI). Four different accumulation time scales of SPEI were used (30, 90, 180, and 365 days) to capture short-, medium-, and long-term hydroclimatic conditions. Statistical significance was assessed at the 0.05 level ($p < 0.05$), with results categorised as $p < 0.001$, $p < 0.01$, $p < 0.05$, and non-significant ($p \geq 0.05$).

2.7 Event-based and high-flow load analysis

Since water chemistry sampling is performed at a lower frequency than flow measurements (daily), linear interpolation was applied to the concentration data to generate a continuous daily time series. Daily nutrient loads were calculated by combining daily discharge with interpolated nutrient concentrations.

2.7.1 Exploratory high-flow screening

Initially, as an exploratory step, a 90th percentile high-flow threshold was applied to identify high-flow conditions (red dotted line, Figure 2). This method serves as a static statistical threshold, isolating only the top 10% of all recorded discharge values during two wet and two dry years across catchments. While this provides a preliminary comparison of nutrient export during high-flow peaks in wet and dry years, it is a rigid limit that does not account for hydrological processes or the duration of individual storms. Results from this screening are presented in the Appendix 5: Table A2.

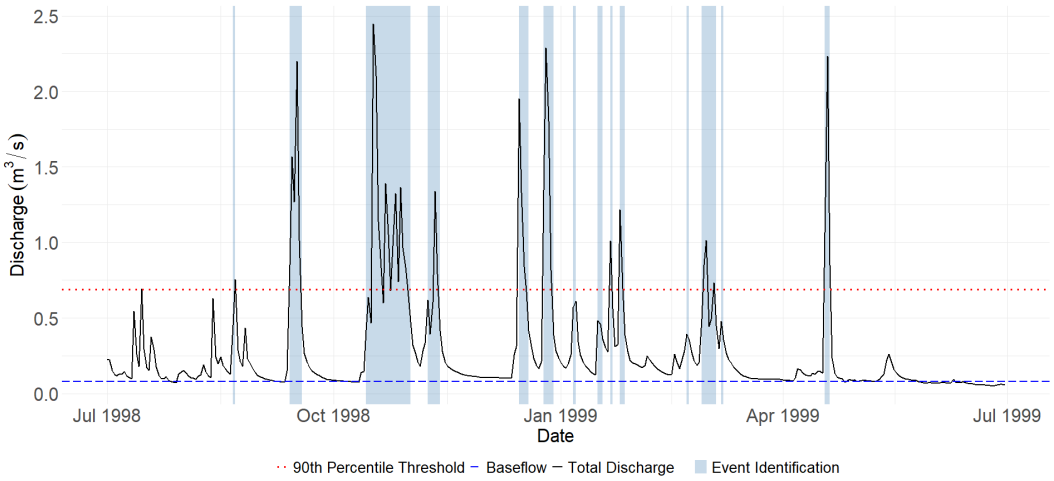

Figure 2. Representative hydrograph for catchment N34 during the wet agrohydrological year 1998/1999, illustrating the difference between identification methods. Shaded blue areas represent events identified via the Event identification method and the red dotted line indicates the 90th percentile threshold. The dashed line represents the baseflow event limit of 0.08 m^3/s calculated using grwat.

2.7.2 Baseflow separation

The separation of baseflow was conducted with the package *grwat* (Samsonov 2025) that is a processed-based algorithm used to distinguish quick flow events in R (R Core Team 2024). Every catchment had its own baseflow calculated for the whole study period. This step is a prerequisite for event identification, as it defines the "floor" of the hydrograph (dashed blue line, Figure 2). This is important in event identification to identify when the flow has returned to baseflow levels, to avoid misidentifying an entire wet season as a single event, ensuring that only true hydrological pulses are isolated.

2.7.3 Event identification

The identification of specific events was calculated using a Python script (Lannergård et al. 2021). Unlike the statistical 90th percentile threshold, the script defines event boundaries by identifying periods where discharge rises above and subsequently returns to catchment-specific baseflow levels (shaded blue area, Figure 2).

Each event is therefore defined as a continuous period of elevated discharge, bounded by the transition from baseflow to quick flow and back to baseflow. For each identified event, nutrient loads were aggregated based on the interpolated daily concentration and discharge data. This approach allows for a more accurate quantification of nutrient export at the event scale and enables comparison of event-driven transport dynamics across catchments and hydrological conditions.

3. Results

3.1 Long-term hydrological characterisation

The SPEI analysis for the period 1989 –2025 identified several distinct episodes of significant hydrological stress across the study catchments I28, N34, and M42 (Figure 3, Figure 4 and Figure 5 respectively). While some events occurred simultaneously at all sites, others were site-specific, highlighting differences in site specific hydrological conditions and catchment characteristics. By calculating the index at 1, 3, 6, and 12-month timescales, both short-term soil moisture fluctuations and long-term deficits in the climatic water balance were captured.

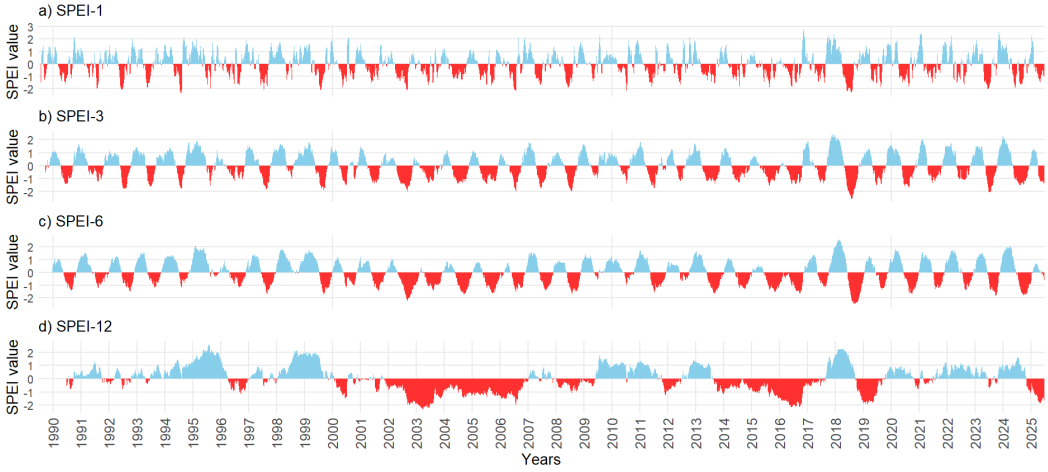

Figure 3. Multi-timescale SPEI for catchment I28 (1989–2025), shown at (a) 1-month, (b) 3-month, (c) 6-month, and (d) 12-month accumulation periods. Blue values represent wet conditions (SPEI > 0), while red values represent dry conditions (SPEI < 0). Increasing timescale smooths short-term variability and highlights longer-term hydrological drought persistence, with SPEI-12 (d) representing integrated water balance anomalies relevant for hydrological stress.

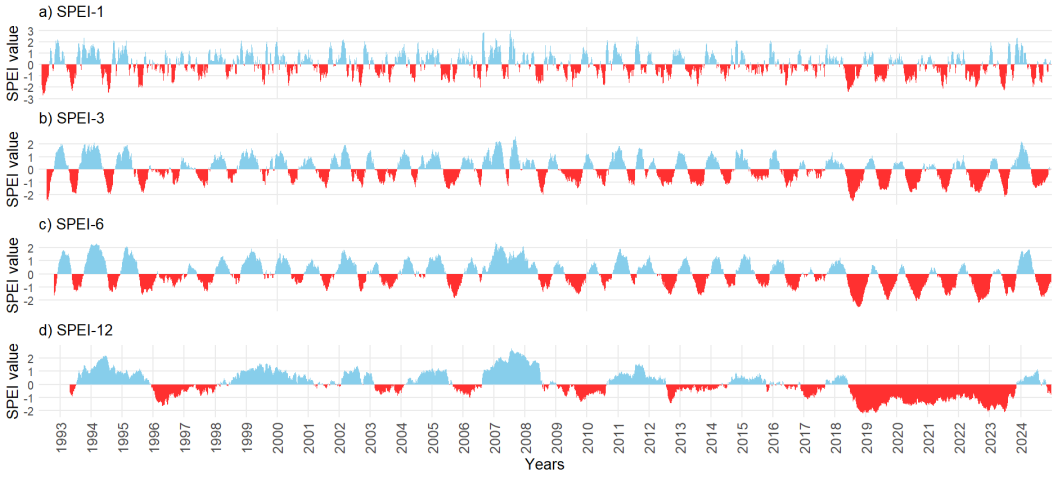

Figure 4. Multi-timescale SPEI for catchment M42 (1992–2024), shown at (a) 1-month, (b) 3-month, (c) 6-month, and (d) 12-month accumulation periods. Blue values represent wet conditions (SPEI > 0), while red values represent dry conditions (SPEI < 0). Increasing timescale smooths short-term variability and highlights longer-term hydrological drought persistence, with SPEI-12 (d) representing integrated water balance anomalies relevant for hydrological stress.

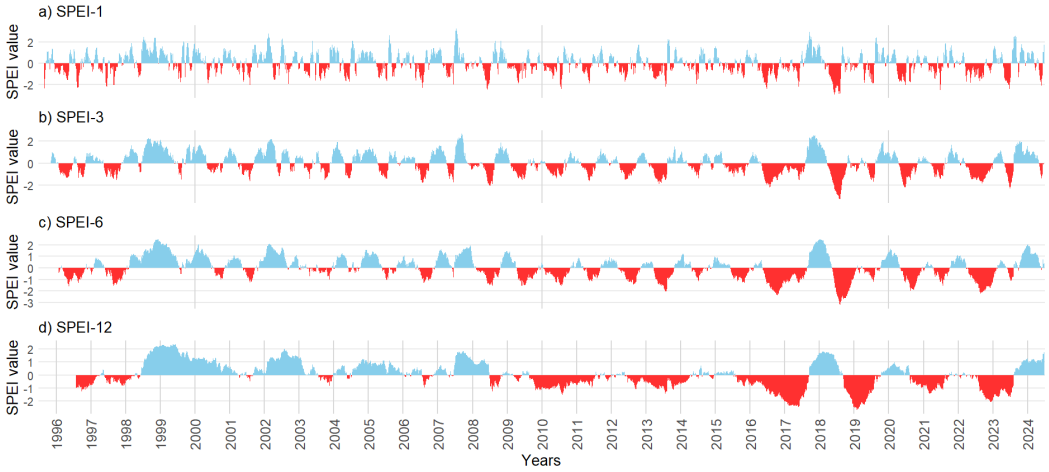

Figure 5. Multi-timescale SPEI for catchment N34 (1995–2024), shown at (a) 1-month, (b) 3-month, (c) 6-month, and (d) 12-month accumulation periods. Blue values represent wet conditions (SPEI > 0), while red values represent dry conditions (SPEI < 0). Increasing timescale smooths short-term variability and highlights longer-term hydrological drought persistence, with SPEI-12 (d) representing integrated water balance anomalies relevant for hydrological stress.

SPEI1-value for all catchments (Figure 3a, Figure 4a and Figure 5a), reached -2 in the second part of 2018, indicating extreme drought. Likewise, it was observed in the winter of 1999 where the SPEI-value exceeded 1.5 in SPEI1 for all catchments (Figure 3a, Figure 4a and Figure 5a). In catchment M42 (Figure 4d) the period

2019-2024 represented a drought period and 2002-2007 was identified as a drought period (Figure 3d).

3.2 Annual nutrient loads

TN loads were lowest for I28 (I28: 1672 ± 602 kg/km²/year) and N34 showed a larger variability (N34: 3428 ± 1160 kg/km²/year) compared to M42 (M42: 2848 ± 1002 kg/km²/year) (Figure 6). Complete loads for TN and TP during study periods at each catchment is found in Appendix 4: Table A1. Catchment I28 showed the highest number of dry years (n = 7), while M42 and N34 each had four dry years. In contrast, wet years were most frequent in I28 (n = 9), followed by N34 (n = 5) and M42 (n = 1). M42 had 18 years included in the analysis, N34 had 29 years and I28 had 36 years.

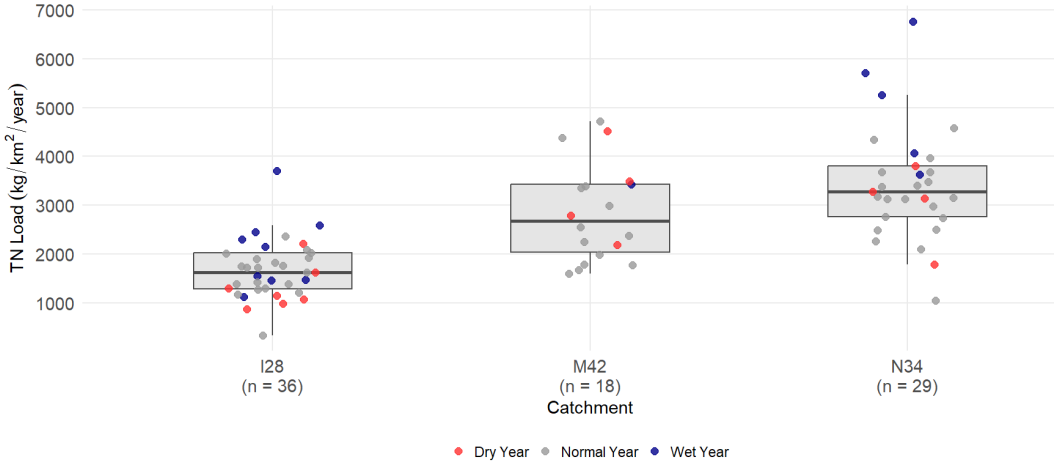

Figure 6. Boxplots over annual TN loads across catchments, each point represents annual load for one agrohydrological year and the different colours on the dot represents if it was identified as a whole year either, wet, dry or normal. Dry years: red (mean SPEI < −1), normal years: grey (−1 ≤ mean SPEI ≤ 1), and wet years: blue (mean SPEI > 1). The horizontal line represents the median, the box indicates the 25th–75th percentile, and the whiskers extend to 1.5 times the interquartile range.

Annual TP loads were of similar magnitude across catchments: I28 (26.0 ± 16.6 kg/km²/year), M42 (44.3 ± 18.9 kg/km²/year), and N34 (36.3 ± 24.7 kg/km²/year). However, N34 displayed the highest interannual variability. (Figure 7).

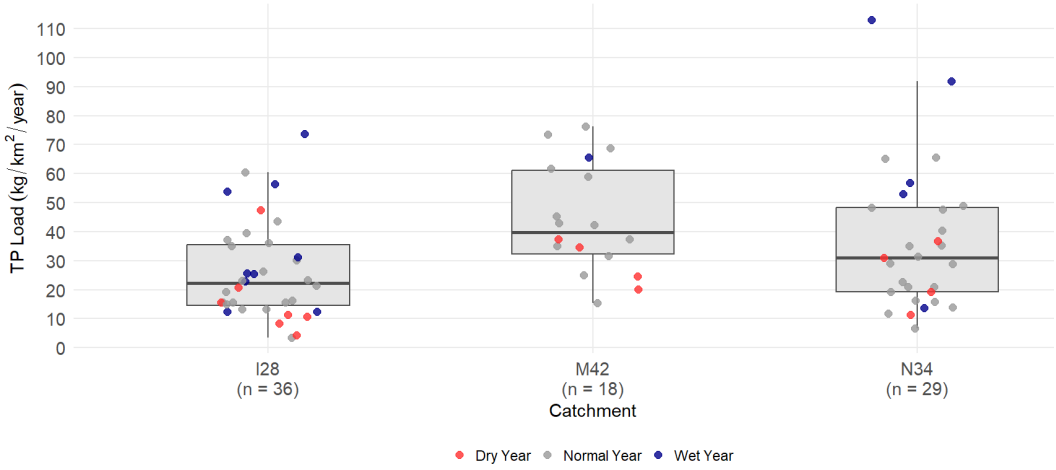

Figure 7. Boxplots over annual TP loads across catchments, each point represents annual load for one agrohydrological year and the different colours on the dot represents if it was identified as a whole year either, wet, dry or normal. Dry years: red (mean SPEI < −1), normal years: grey (−1 ≤ mean SPEI ≤ 1), and wet years: blue (mean SPEI > 1). The horizontal line represents the median, the box indicates the 25th–75th percentile, and the whiskers extend to 1.5 times the interquartile range.

Some nutrient load peaks were identified simultaneously across catchments. N34 has the highest annual load in year 1998/1999 (Figure 8). The year 1995/1996 had the lowest TN loads for I28: 336.9 kg/km^2 and N34: 1051.9 kg/km^2.

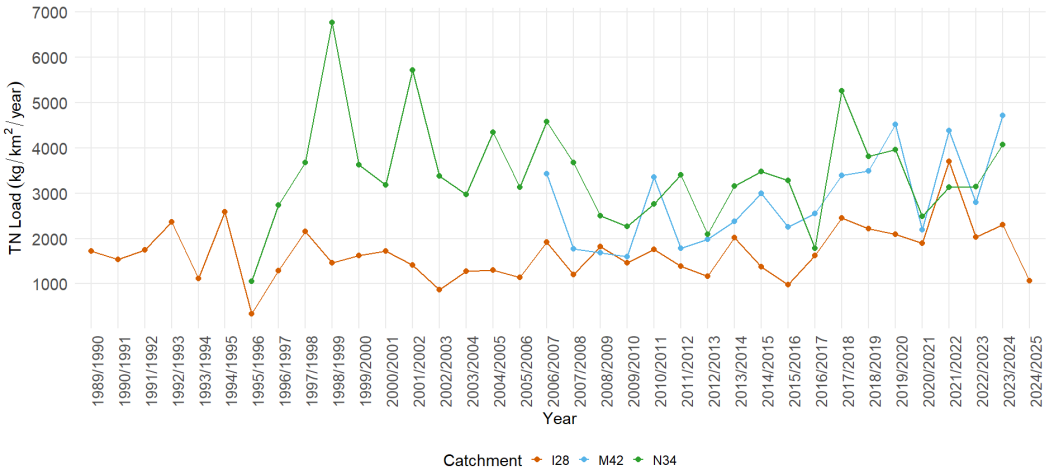

Figure 8. Annual total nitrogen (TN) loads (kg/km²/year) for the studied catchments (I28, M42 and N34) over the study period, based on agrohydrological years. Each line represents one catchment, as indicated in the legend.

The year 1998/1999 was characterised by persistently wet conditions, as indicated by positive SPEI values, at all sites (Figure 3d, Figure 4d and Figure 5d). During this year, TP and TN loads were substantially elevated for N34, reaching 113 kg/km² TP and up to 6766 kg/km² TN (Figure 8 and Figure 9).

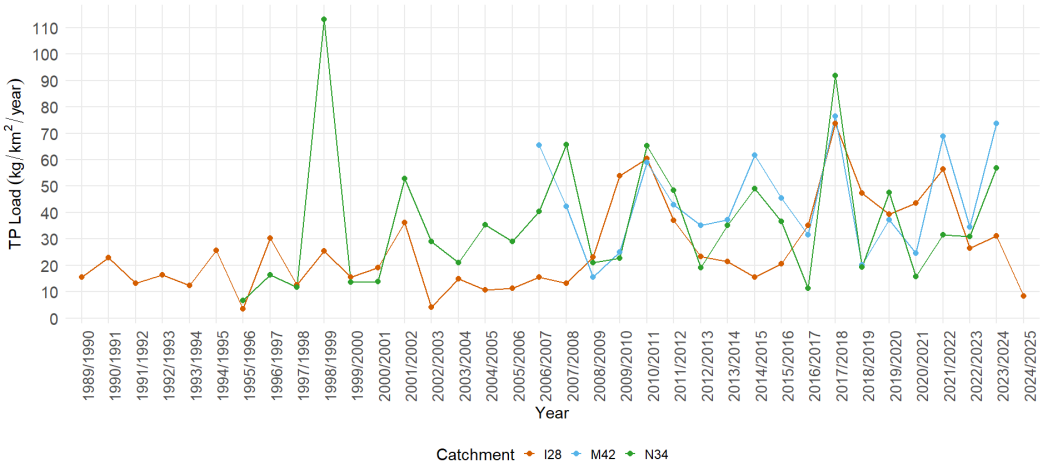

Figure 9. Annual total phosphorus (TP) loads (kg/km²/year) for the studied catchments (I28, M42 and N34) over the study period, based on agrohydrological years. Each line represents one catchment, as indicated in the legend.

Spearman's rank correlation analysis revealed varying relationships between different timescales in SPEI and the proportional contribution to annual nutrient loads across catchments (Table 2). In I28, the strongest correlations were observed at SPEI-1, for TN ($\rho = 0.32$, $p < 0.001$, Table 2) and TP ($\rho = 0.24$, $p < 0.001$, Table 2). A shift from positive to negative correlations was observed with increasing SPEI time scale, particularly for TN at SPEI-6. In M42, weak to moderate correlations were observed, with positive relationships at shorter SPEI time scales and negative correlations at longer time scales for both TN and TP. Several of these correlations were statistically significant ($p < 0.05$). In N34, correlations were generally weak, with predominantly positive associations at shorter time scales, while long-term SPEI showed no significant relationships. Overall, stronger and more consistent relationships were observed at shorter SPEI time scales, while longer time scales showed weaker or mixed associations depending on catchment and nutrient type.

Table 2. Spearman's rank correlation coefficients (ρ) and associated significance values (p) describing the relationship between the proportional contribution of individual hydrological events to total annual loads (%) and the Standardised Precipitation-Evapotranspiration Index (SPEI) at multiple time scales (30, 90, 180, and 365 days). Results are presented for total nitrogen (TN) and total phosphorus (TP) across the three study catchments: I28, M42 and N34.

Catchment		SPEI-1	SPEI-3	SPEI-6	SPEI-12
I28	TN	ρ=+0.32 (p<0.001)***	ρ=+0.15 (p=0.018)*	ρ=−0.20 (p=0.002)**	ρ=−0.08 (p=0.198)
	TP	ρ=+0.24 (p<0.001)***	ρ=+0.16 (p=0.013)*	ρ=−0.08 (p=0.224)	ρ=−0.07 (p=0.275)
M42	TN	ρ=+0.18 (p=0.005)**	ρ =+0.10 (p=0.138)	ρ=−0.14 (p=0.033)*	ρ=−0.19 (p=0.005)**

	TP	ρ=+0.22 (p=0.001)***	ρ =+0.10 (p=0.126)	ρ=−0.14 (p=0.037)*	ρ=−0.17 (p=0.009)**
N34	TN	ρ=+0.22 (p=0.001)***	ρ =+0.13 (p=0.053)	ρ=+0.04 (p=0.580)	ρ=−0.04 (p=0.598)
	TP	ρ=+0.20 (p=0.003)**	ρ=+0.15 (p=0.030)*	ρ=+0.08 (p=0.252)	ρ=+0.01 (p=0.863)

*Significance: *** p < 0.001, ** p < 0.01, * p < 0.05, (ns) p > 0.05.

During the study period in I28 there was no significant trend regarding TN concentrations, until about 2012 when an increasing trend for about three years was identified (Figure 10).

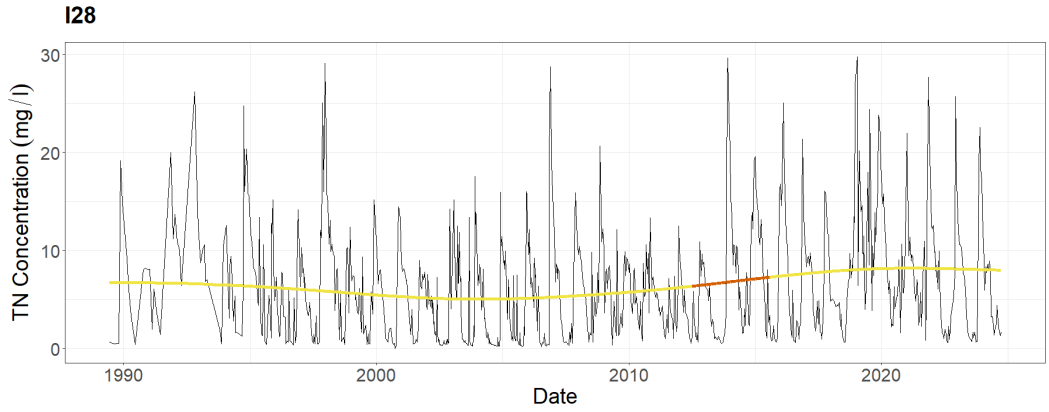

Figure 10. Trend curve for total nitrogen (TN) concentration (mg/l) in I28 (1989 – 2024) produced by a generalised additive model (GAM). Colour indicates periods with significant trends, decreasing (blue), increasing (red), and no significant trend (yellow), based on the first derivative of the smooth term (95% confidence interval). Observed values are shown as black points/lines, and the smooth curve represents the fitted long-term trend including seasonal variation.

During the study period in I28 there was no significant trend for TP concentrations, until about 2008 when there was a small increase in the concentrations but still no significant trend. In year 2015 there was a larger increase up until 2019 identified as an increasing trend that later stagnated and then between 2021 and 2024 a decreasing trend was identified ending at the same values as before the increase in 2015 (Figure 11).

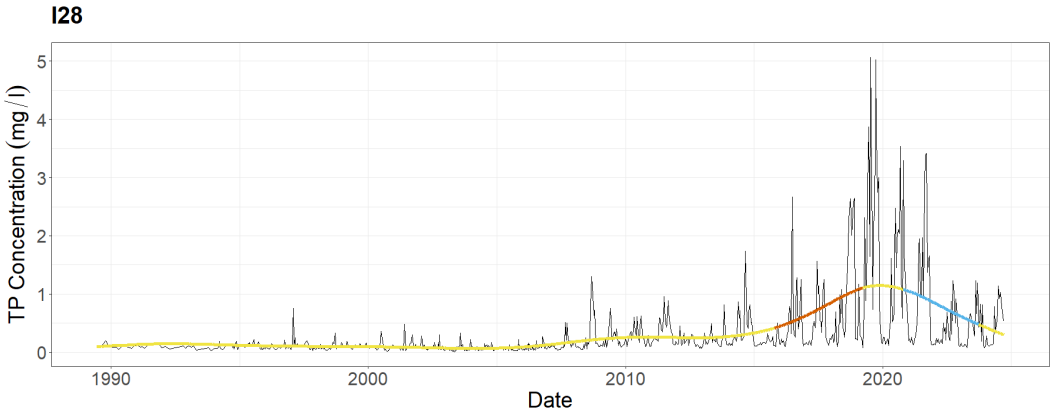

Figure 11. Trend curve for total phosphorus (TP) concentration (mg/l) in I28 (1989 – 2024) produced by a generalised additive model (GAM). Colour indicates periods with significant trends, decreasing (blue), increasing (red), and no significant trend (yellow), based on the first derivative of the smooth term (95% confidence interval). Observed values are shown as black points/lines, and the smooth curve represents the fitted long-term trend including seasonal variation.

Annual TN concentration in M42 had an overall smooth pattern, with multiple decreasing and increasing trends but for the most part no significant trends (Figure 12). Annual TN load in N34 had a smoother pattern with less variation (Figure 13) compared to M42 (Figure 12).

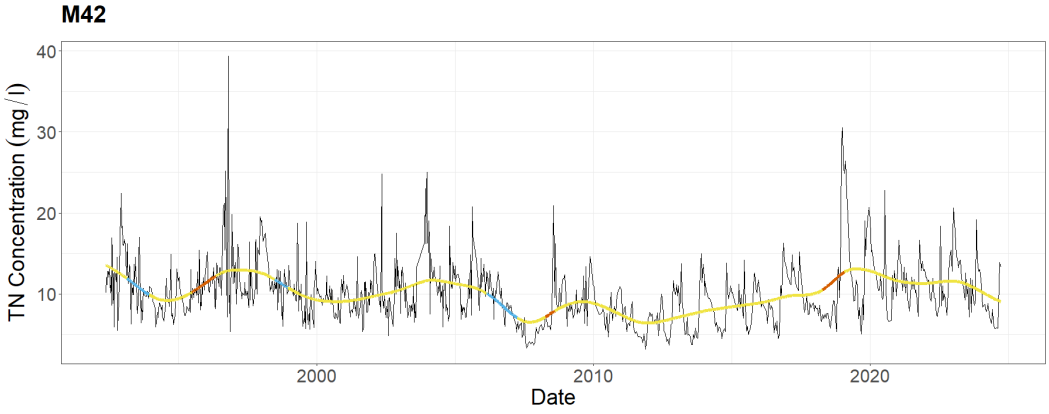

Figure 12. Trend curve for total nitrogen (TN) concentration (mg/l) in M42 (1992 – 2024) produced by a generalised additive model (GAM). Colour indicates periods with significant trends, decreasing (blue), increasing (red), and no significant trend (yellow), based on the first derivative of the smooth term (95% confidence interval). Observed values are shown as black points/lines, and the smooth curve represents the fitted long-term trend including seasonal variation.

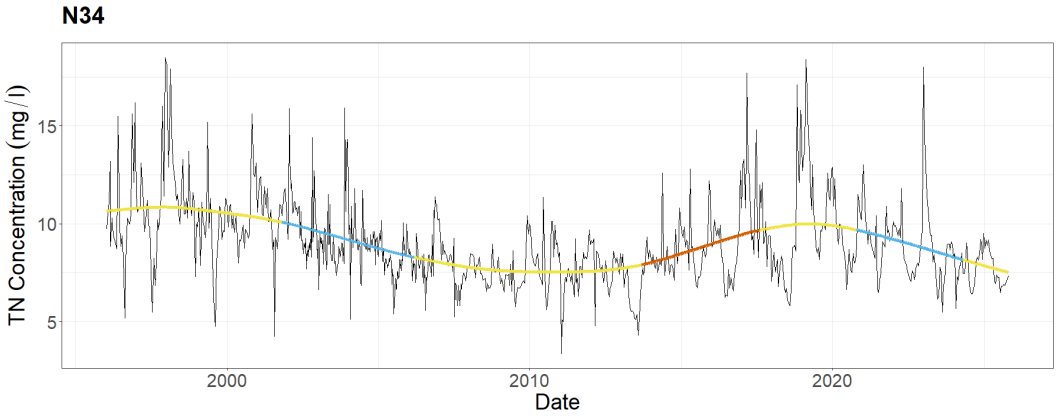

Figure 13. Trend curve for total nitrogen (TN) concentration (mg/l) in N34 (1996-2024) produced by a generalised additive model (GAM). Colour indicates periods with significant trends, decreasing (blue), increasing (red), and no significant trend (yellow), based on the first derivative of the smooth term (95% confidence interval). Observed values are shown as black points/lines, and the smooth curve represents the fitted long-term trend including seasonal variation.

For loads, the general pattern for all catchments were no significant trends, see Appendix 3: Figure A1, A2, A3 and A4). However, the TN load in N34 had a general decreasing trend during the study period (Figure 14) and the TP load in M42 had a general increasing trend during the study period (Figure 15). The annual TP concentration for M42 however had no significant trends except a small increase 1996-2000 (Figure 16).

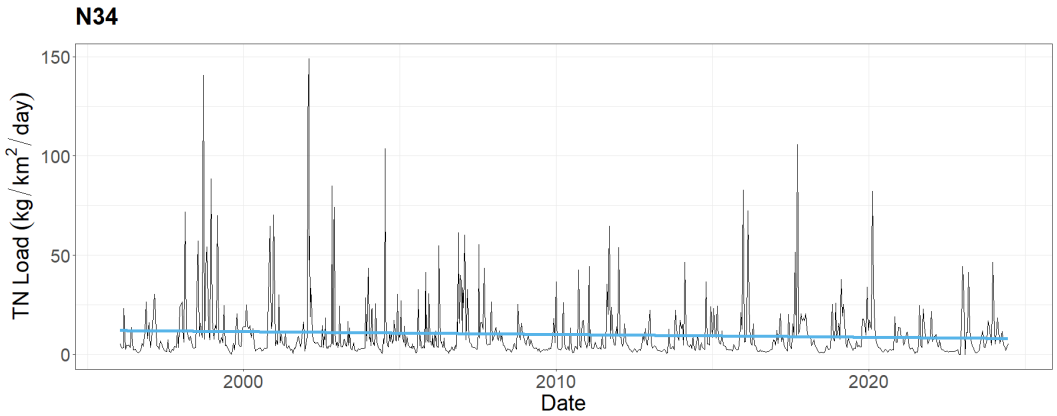

Figure 14. Trend curve for total nitrogen (TN) load (kg/km²/day) in N34 (1996-2024) produced by a generalised additive model (GAM). Colour indicates periods with significant trends, decreasing (blue), increasing (red), and no significant trend (yellow), based on the first derivative of the smooth term (95% confidence interval). Observed values are shown as black points/lines, and the smooth curve represents the fitted long-term trend including seasonal variation.

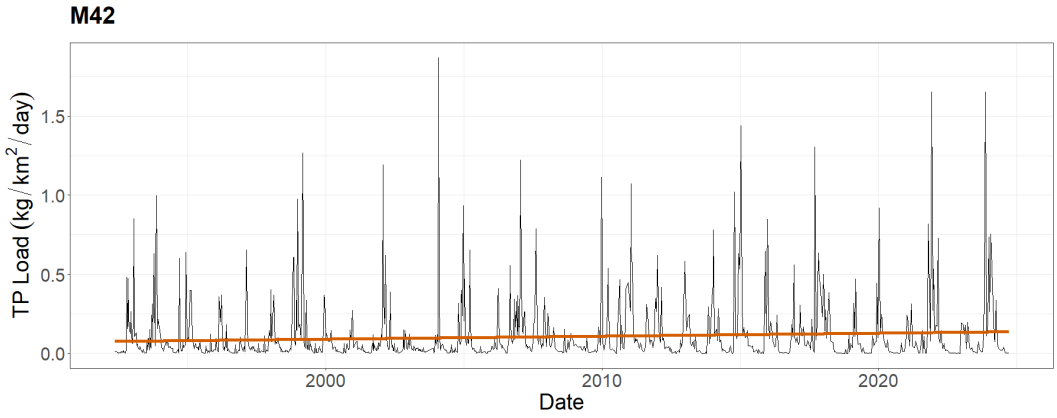

Figure 15. Trend curve for total phosphorus (TP) load (kg/km²/day) in M42 (1992 – 2024) produced by a generalised additive model (GAM). Colour indicates periods with significant trends, decreasing (blue), increasing (red), and no significant trend (yellow), based on the first derivative of the smooth term (95% confidence interval). Observed values are shown as black points/lines, and the smooth curve represents the fitted long-term trend including seasonal variation.

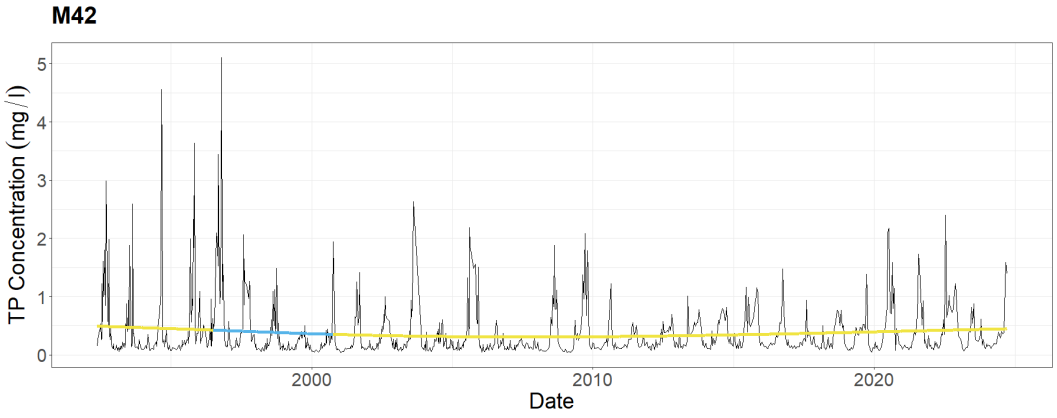

Figure 16. Trend curve for total phosphorus concentration mg/l (TP) in M42 (1992 – 2024) produced by a generalised additive model (GAM). Colour indicates periods with significant trends, decreasing (blue), increasing (red), and no significant trend (yellow), based on the first derivative of the smooth term (95% confidence interval). Observed values are shown as black points/lines, and the smooth curve represents the fitted long-term trend including seasonal variation.

3.3 Nutrient responses to extreme events

Years characterised as wet in SPEI-12 (Figure 3d, Figure 4d and Figure 5d) had more detected events and years characterised as dry had fewer events detected (Table 3). I28 and N34 catchment's dry years had a lower TN and TP load compared to the wet year in the same catchment (Table 3). M42 on the other hand had similar loads for the wet and the dry years. The baseflow for the catchments

were calculated to 0.08 m3/s (N34), 0.03 m3/s (M42) and 0.01 m3/s (I28) with grwat (Samsonov 2025).

Table 3. High-flow event frequency and associated nutrient export (TN and TP) for catchments M42, N34, and I28. Results are categorised by wet and dry agrohydrological years as defined by SPEI-12. Event identification is based on regionalised quick flow thresholds for each catchment.

Catchment	Agrohydrological year	Characterised	Number of events	TN of annual load (%)	TP of annual load (%)
I28	1994/1995	Wet	15	71	63
I28	2005/2006	Dry	6	21	14
M42	2007/2008	Wet	11	62	56
M42	2023/2024	Dry	8	60	56
N34	1998/1999	Wet	11	63	71
N34	2016/2017	Dry	2	33	35

The agrohydrological year-scale analysis highlighted how extreme hydrological conditions strongly influenced TN and TP loads, with distinct responses observed between nutrients and catchments. Catchment I28 experienced a longer meteorological drought between 2002-2007, 662 days during this period had SPEI-3 < -1.0 (Figure 3d). These days represented 30% of all days during the period, however the total TN load during these days was 0.2% and total TP load was 0.9% (Appendix 8: Table A5). When zooming in to the 3-month scale (Figure 3b), TN loads increased simultaneously with blue peaks (Figure 17).

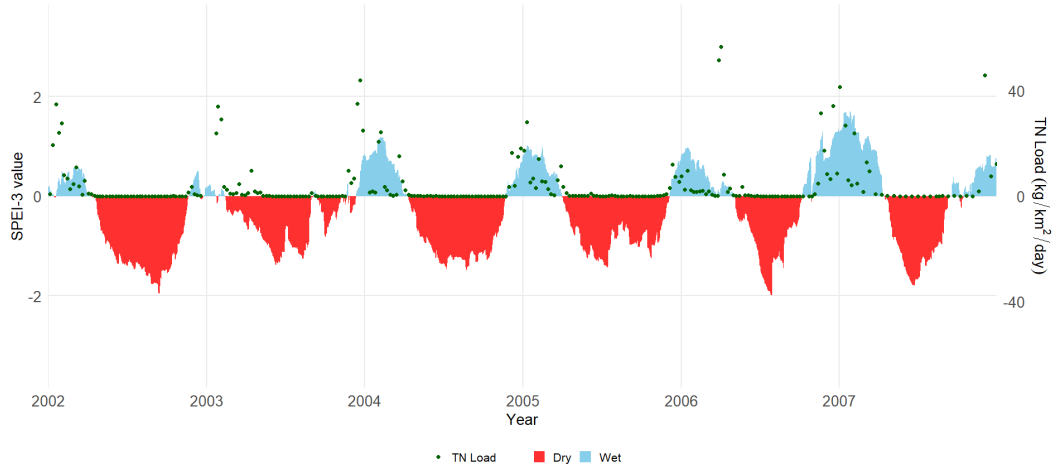

Figure 17. Temporal variation in total nitrogen (TN) load (kg/km²/day) and (SPEI-3) for catchment I28 during a dry period (2002–2007). TN load is shown as green points, while SPEI-3 is represented by coloured values, where negative values (SPEI < 0) indicate dry conditions (red) and positive values (SPEI > 0) indicate wet conditions (blue) relative to the long-term average.

Zooming in further, the year 2005 at catchment I28 demonstrated the critical role of hydrological first-flush events. Following a severe meteorological drought, 78 days of SPEI-3 < -1.0 was established, the spring flood events triggered an export of estimated accumulated TN (Figure 18). The event identification method found six events, these events stood for 21% of the annual TN load and 14% of the annual TP load (Table 3).

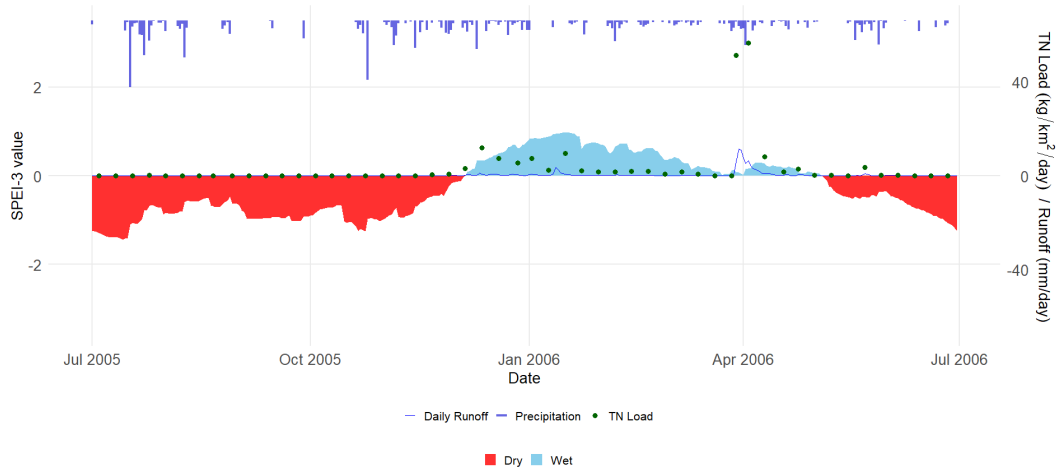

Figure 18. Temporal variation in total nitrogen (TN) load (kg/km²/day) and (SPEI-3) for catchment I28 during the 2005/2006 agrohydrological year. TN load is shown as green points, while SPEI-3 is represented by coloured values, where negative values (red) indicate dry conditions (SPEI < 0) and positive values (blue) indicate wet conditions (SPEI > 0) relative to the long-term average. Precipitation (mm/day) is displayed as an inverted hyetograph from the top axis. Daily runoff (mm/day) is shown as a continuous blue line.

Catchment N34 had a longer wet period during 1998-2002, SPEI-3 values > 1.5 for 294 days during this period (Figure 5d). Those days stood for 16% of all the days during the period however the annual TN and TP load was 31% and 54% (Appendix 8: Table A5). The results for catchment N34 showed a strong temporal connection between hydrological status and TN export (Figure 19). Peak TN loads consistently coincided with periods of positive SPEI-3 values, particularly during the winters of 1999 and 2001, when the index indicated severely wet conditions (Figure 19). Similarly, TP loads during the winter 1998 coincided with higher SPEI-3 values (Figure 20). In contrast, during the winter of 2000 the same was not observed, potentially due to lower SPEI-3 value (Figure 20). A distinct seasonal pattern was evident, with minimal TN export during dry summer periods, followed by a rapid increase during autumn and winter (Figure 19).

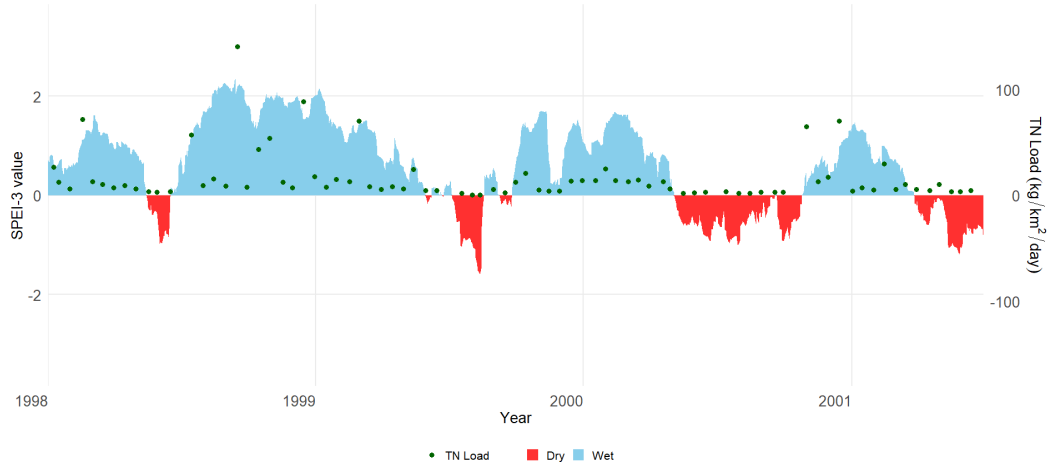

Figure 19. Temporal variation in total nitrogen (TN) load (kg/km²/day) and (SPEI-3) for catchment N34 during a wet period (1998-2002). TN load is shown as green points, while SPEI-3 is represented by coloured values, where negative values (SPEI < 0) indicate dry conditions (red) and positive values (SPEI > 0) indicate wet conditions (blue) relative to the long-term average.

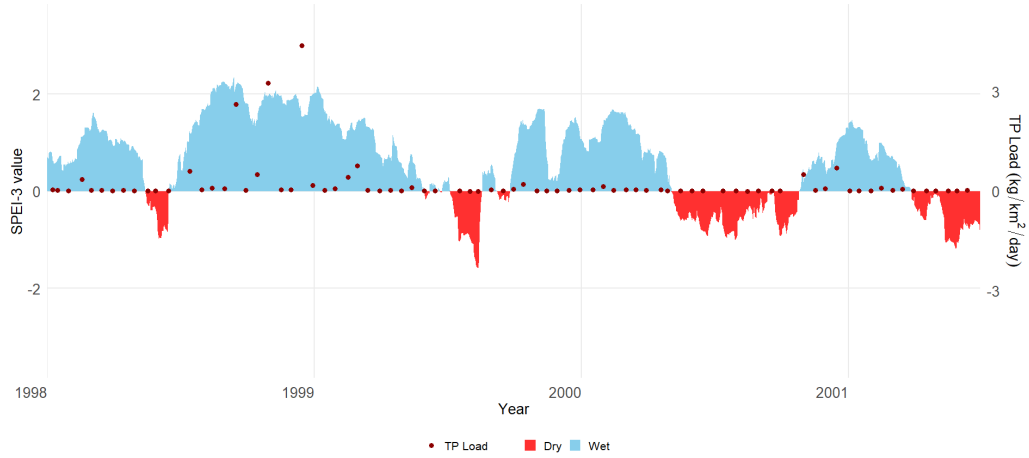

Figure 20. Temporal variation in total phosphorus (TP) load (kg/km²/day) and (SPEI-3) for catchment N34 during a wet period (1998-2002). TP load is shown as dark red points, while SPEI-3 is represented by coloured values, where negative values (SPEI < 0) indicate dry conditions (red) and positive values (SPEI > 0) indicate wet conditions (blue) relative to the long-term average.

During year 1998/1999 at catchment N34, nutrient export was controlled by hydrological conditions, with SPEI-3 values > 1.5 for 168 days, 95 days consistently, of the year (Figure 21). TN load showed a relatively continuous pattern, with elevated values throughout the year and increases during periods of high runoff. TP load showed a more episodic pattern, characterised by low background levels of TP and high peaks matching with high runoff (Figure 22). During this year the 11 events stood for 63% of the annual TN load and 71% of the annual TP load.

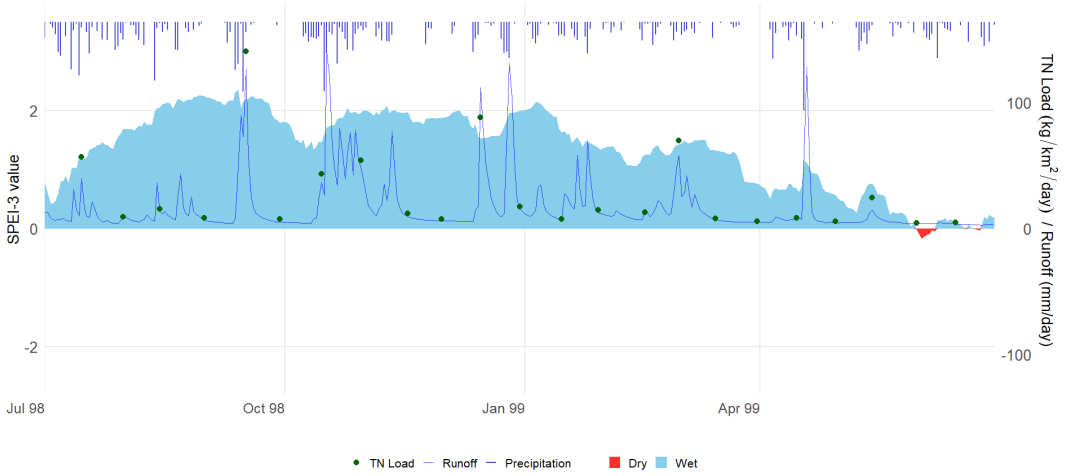

Figure 21. Temporal variation in total nitrogen (TN) load (kg/km²/day) and (SPEI-3) for catchment N34 during the 1998/1999 agrohydrological year. TN load is shown as green points, while SPEI-3 is represented by coloured values, where negative values (red) indicate dry conditions (SPEI < 0) and positive values (blue) indicate wet conditions (SPEI > 0) relative to the long-term average. Precipitation (mm/day) is displayed as an inverted hyetograph from the top axis. Daily runoff (mm/day) is shown as a continuous blue line.

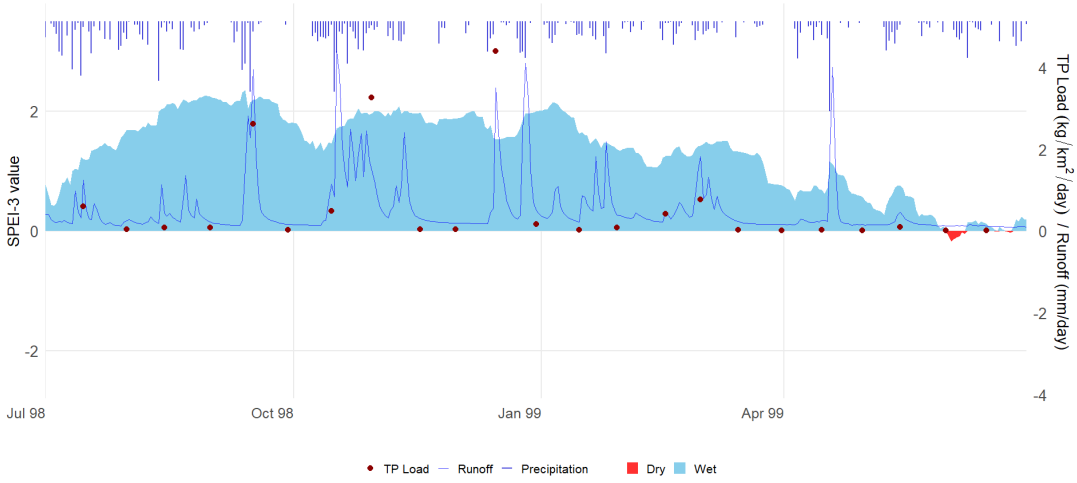

Figure 22. Temporal variation in total phosphorus (TP) load (kg/km²/day) and (SPEI-3) for catchment N34 during the 1998/1999 agrohydrological year. TP load is shown as dark red points, while SPEI-3 is represented by coloured values, where negative values (red) indicate dry conditions (SPEI < 0) and positive values (blue) indicate wet conditions (SPEI > 0) relative to the long-term average. Precipitation (mm/day) is displayed as an inverted hyetograph from the top axis. Daily runoff (mm/day) is shown as a continuous blue line.

The 2018–2025 period at station M42 was characterised by frequent and sustained intervals of negative SPEI-3 values, with the most pronounced deficit occurring in 2018 (Figure 23). 485 days during this period had SPEI-3 < -1.5, 19% of the whole

period. The TN and TP annual load was during those days 0.2% and 0.8% (Appendix 8: Table A5). TN load showed a relatively continuous pattern, with almost zero TN loads throughout the year and during periods of positive SPEI-3 values TN loads increased (Figure 23). Specifically, the transition from negative (red) SPEI-3 values to positive (blue) SPEI-3 values was associated with high TN loads.

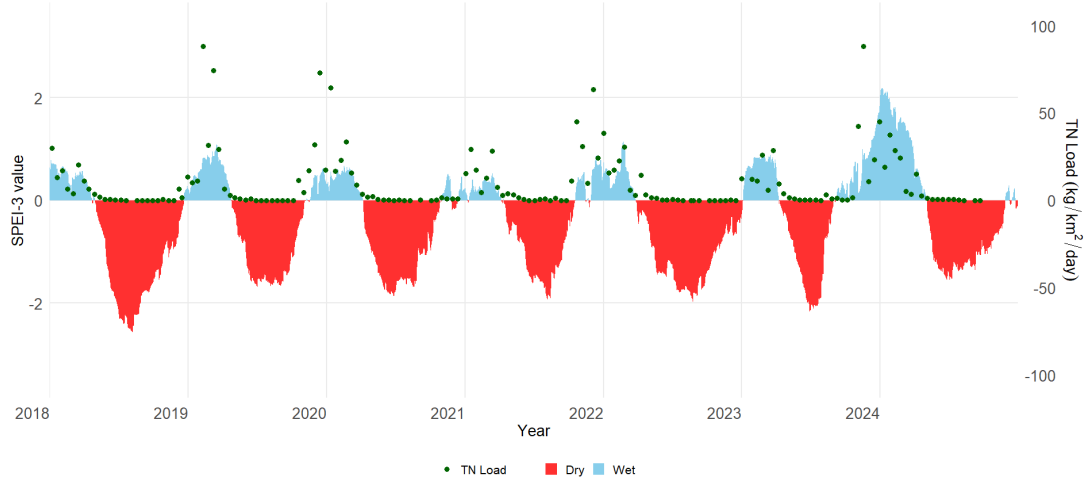

Figure 23. Temporal variation in total nitrogen (TN) load (kg/km²/day) and (SPEI-3) for catchment M42 during a dry period (2018-2025). TN load is shown as green points, while SPEI-3 is represented by coloured values, where negative values (SPEI < 0) indicate dry conditions (red) and positive values (SPEI > 0) indicate wet conditions (blue) relative to the long-term average.

During the first quarter of the 2023/2024 year, several precipitation events were recorded, however the SPEI-3 remained negative, SPEI-3 < -1.5 for 36 days of the year (Figure 24). Throughout this period, daily runoff and TN load measurements remained at baseline levels despite the recorded rainfall. Both daily runoff and TN loads increased simultaneously in late autumn, coinciding with the shift to positive SPEI-3 values. Peak TN loads during this period were recorded at values exceeding 80 kg/km²/day (Figure 24). During this year the eight events stood for 60% of the annual TN load and 56% of the annual TP load (Table 3).

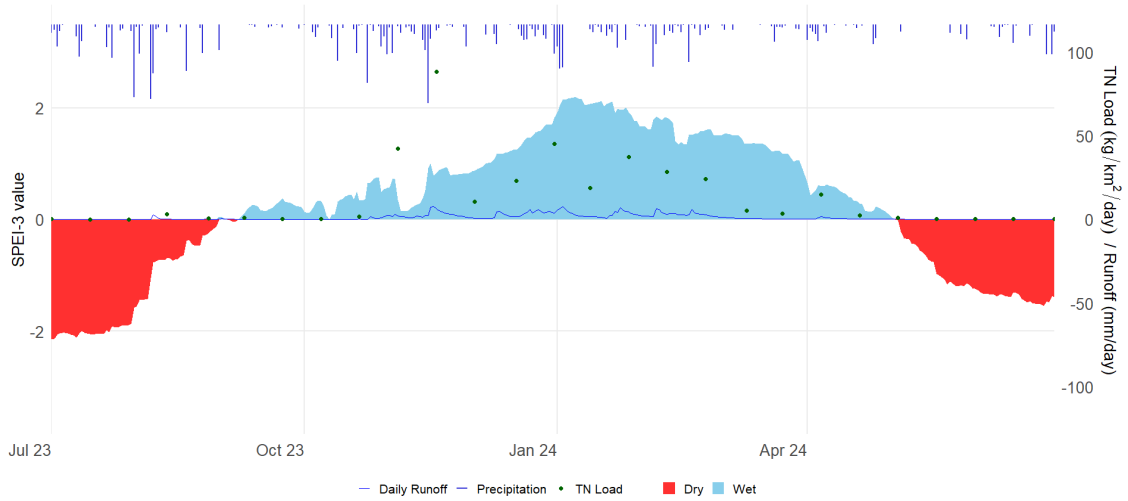

Figure 24. Temporal variation in total nitrogen (TN) load (kg/km²/day) and (SPEI-3) for catchment M42 during the 2023/2024 agrohydrological year. TN load is shown as green points, while SPEI-3 is represented by coloured values, where negative values (red) indicate dry conditions (SPEI < 0) and positive values (blue) indicate wet conditions (SPEI > 0) relative to the long-term average. Precipitation (mm/day) is displayed as an inverted hyetograph from the top axis. Daily runoff (mm/day) is shown as a continuous blue line.

4. Discussion

4.1 Main findings and hydrological controls

Across all catchments, nutrient export is primarily event-driven rather than controlled by long-term concentration trends. Positive SPEI values during wet years indicate prolonged moisture surplus and increased hydrological connectivity within the catchments, as observed for N34 during 1998/1999 (Figure 21 and Figure 22). Hydrological connectivity refers to the of flow pathways that enable water and dissolved or particulate substances to move from source areas within the catchment to the stream network. Increased runoff enhances hydrological connectivity, mobilizing P from surface and near-surface sources. In contrast, N dynamics are often governed by dilution effects, where increased discharge leads to lower concentrations but still elevated total loads due to higher water volumes (Chen et al. 2026).

Overall, the results indicate that extreme wet periods substantially increase both TN and TP loads in agricultural catchments, primarily through enhanced runoff and hydrological connectivity. However, the dominant mobilisation mechanisms differed between the two nutrients. TN loads appeared to be associated with sustained subsurface transport and elevated discharge volumes, whereas TP loads were more linked to short-term event dynamics and mobilisation of PP during intense runoff events. In contrast, dry periods generally reduced annual nutrient export due to lower runoff volumes and reduced connectivity. However antecedent drought conditions may increase the risk of strong nutrient flushing during subsequent rainfall events.

Overall, periods with SPEI-3 values exceeding ±1.5 represented a disproportionally large share of annual nutrient export across all catchments, particularly during prolonged wet periods in N34 and post-drought rewetting events in I28 and M42.

4.2 Contrasting TN and TP mobilisation patterns

In Sweden, there have been intensive mitigation programmes to control N leaching and TN loads decreased until 2010 for I28 and N34 (Figure 8) aligning with other studies (e.g. Kyllmar et al. 2023). However, recent years increase in TN loads could be due to a lower percentage of farmers growing catch crops. The decline in catch crop cultivation was not compensated for by increased cultivation of autumn-sown crops or ley in these catchments (Linefur et al. 2024). In addition, it could depend on weather variations.

During wet years, the identified events accounted for more than 60% of the annual TN load in I28 and M42 (Table 3). Positive SPEI values indicate prolonged wet conditions and increased hydrological connectivity, it suggests that TN exports were primarily driven by sustained hydrological transport, likely dominated by dissolved forms moving through subsurface pathways (Jiang et al. 2010). In another study on these catchments, precipitation appeared to be a highly significant indicator of TN loads in N34 and I28 (Ezzati et al. 2023). This could explain why the annual load for M42 does not differ as much between dry and wet years as for N34 and I28 (Table 3). The dominant soil texture in these catchments is loam/sandy loam that likely facilitate subsurface transport and tile drainage flow during wet conditions, increasing the export of dissolved N forms. At the same time, prolonged saturation may also enhance denitrification within the soil profile (Ezzati et al. 2023).

Overall, the TN dynamics observed across the catchments suggest that TN export was primarily controlled by sustained hydrological transport processes rather than isolated runoff events. Positive SPEI conditions likely enhanced subsurface connectivity and tile drainage flow, resulting in prolonged periods of elevated dissolved TN export. At the same time, antecedent drought conditions may have increased the availability of mineralised N, contributing to enhanced mobilisation during subsequent rewetting events.

During dry years, lower runoff volumes reduced hydrological connectivity and consequently lowered annual TN export in I28 and N34. However, antecedent drought conditions may also influence subsequent TN mobilisation. Following dry periods, enhanced mineralisation of organic N can increase the availability of dissolved N forms in the soil profile. After the dry season of 2018 the low soil water content could have enhanced mineralisation of organic N (Kyllmar et al. 2023).

Furthermore, during prolonged drought, crop growth is severely limited, leading to a reduced uptake of applied N fertilizers. This unused N remains in the soil profile and is highly susceptible to leaching when precipitation returns. The timing of these extreme weather events is also a critical factor; intense rainfall during late summer or autumn, when the soil is bare and active crop uptake has ceased, poses a significantly higher risk for N flushing compared to events occurring during the early summer growing season. The annual TN load in I28 and N34 during the dry years (Table 3) was lower than for the wet years. Although dry years generally resulted in lower annual TN loads, prolonged drought conditions may increase nutrient accumulation and potentially enhancing mobilisation during subsequent rewetting events.

In contrast to TN, TP export appeared to respond more episodically to hydrological extremes and high-flow conditions. While TN transport was characterised by relatively continuous export during wet periods, TP mobilisation was more strongly associated with individual runoff events and rapid hydrological connectivity between source areas and the stream network.

While the results strongly suggest event-driven TP transport, it is important to note that the dominant soil types in these catchments are loam and sandy loam (Table 1), rather than heavy clay. Therefore, the structural vulnerability to pure surface erosion may vary, and rapid subsurface transport could also play a significant role. As highlighted in future recommendations, analysing SS alongside TP would be necessary to fully quantify the exact proportion of erosion-driven PP in these specific areas.

All catchments have a high P-AL class, indicating a large P storage in the soil. However, even if there is a large P storage in the soil it does not automatically lead to large leaching losses. This depends largely on the physical transport mechanisms, how erosion prone the soil is, the soil texture, and the P sorption capacity of the soil (Sharpley et al. 2002). While the results strongly suggest event-driven TP transport, it is important to note that the dominant soil types in these catchments are loam and sandy loam (Table 1), rather than heavy clay. Therefore, the structural vulnerability to pure surface erosion may vary, and rapid subsurface transport could also play a significant role.

The agrohydrological year 1998/1999 in N34 was characterised by strongly positive SPEI-12 values approaching +2, indicating exceptionally wet conditions. An extreme weather event could trigger peaks in TP losses like the peak in N34 in agrohydrological year 1998 (Figure 22). Elevated P export during wet conditions is likely driven by increased runoff, enhanced hydrological connectivity and reduced retention capacity in the soil. Prolonged saturation may also promote the release of P from iron oxides under reducing conditions (Patrick & Jugsujinda 1992).

High-intensity rainfall following a drought period can trigger extreme peaks of TP concentrations in agricultural catchments with peaks with an increase of concentrations up to 1400% compared to non-extreme events (Dupas et al. 2024). The mechanism behind these peaks is driven by an infiltration excess that creates overland flow. This flow can then mobilise surface-near legacy P sources, a process that is predicted to intensify in future climate conditions (Dupas et al. 2024). Although Dupas et al. (2024) investigated concentration responses, similar hydrological mechanisms may also contribute to elevated TP loads through increased runoff volumes.

Miller & Lyon (2021) found that during wetter years significant positive correlations between tile drainage density, runoff and soluble reactive P concentrations was established, these correlations were not found in drier year. Therefore, it is in line with the literature that TP is higher on a wet year like 1998.

The observed reduction in TP transport during dry years in I28 and N34 is likely explained by limited hydrological connectivity and reduced runoff volumes. Lower soil saturation decreases both overland flow and the connectivity between TP source areas and the stream network, effectively stopping the transport of PP. However, prolonged dry conditions may increase the risk of elevated TP mobilisation during subsequent rewetting events. This difference may explain why TP responses appeared more episodic and potentially more sensitive to hydrological extremes and first-flush events.

4.3 The importance of antecedent hydrological conditions and SPEI

Nutrient export in agricultural catchments is strongly controlled by runoff dynamics. Comparing the results from the event identification analysis and the 90% high-flow threshold, reveals that event-based estimates generally reduced estimated nutrient loads during dry years but increased them during wet years. For example, during the wet year in N34 1998/1999, the event-based analysis accounted for 63% of the annual TN load and 71% of the annual TP load, whereas the high-flow threshold method captured only 43% and 59%, respectively. In contrast, during the dry year in I28 2005/2006, the event-based analysis accounted for only 21% of the annual TN load and 14% of the annual TP load, while the high-flow threshold method captured 76% and 83%, respectively (Table 3 and Appendix 5: Table A2). This suggests that the 90% high-flow threshold alone may not fully capture the hydrological dynamics controlling nutrient mobilisation.

The event identification method captures complete hydrological events and therefore reflects the total nutrient export associated with an entire runoff event (Lannergård 2021). In contrast, the 90% high-flow threshold method shows conditions during the highest discharge levels, which may overlook important mobilisation phases, particularly at the beginning of events when accumulated nutrients are rapidly flushed from soils.

A key process underlying these differences is the role of antecedent soil moisture conditions. After dry summer periods, soils typically require a period of rewetting before becoming hydrologically connected to the drainage system. In this rewetting phase, infiltration capacity, preferential flow activation, and surface–subsurface connectivity changes rapidly, meaning that initial rainfall events can generate

disproportionately high nutrient export even before peak discharge is reached. This supports the idea of a potential first-flush effect, particularly for P, where nutrients accumulated during dry periods are rapidly mobilised during the initial stages of runoff events. However, if the soil is severely dry, even a large precipitation event may fail to generate immediate runoff or export because the soil matrix remains undersaturated (Macrae et al. 2009). This threshold effect is evident in the dry year 2023/2024 for M42 (Figure 24).

The wet year of M42 2007/2008 had 32% of annual TN- and 38% of annual TP loads using the 90% high-flow threshold and using the event identification analysis: 62% of annual TN- and 56% of annual TP loads. These differences indicate that nutrient mobilisation is controlled not only by peak discharge magnitude, but also by the temporal development of runoff events, particularly during the rising limb.

This pattern can be further interpreted using SPEI as an indicator of antecedent climatic and soil moisture conditions. SPEI-1 reflects immediate meteorological drought and is likely more closely related to P export events triggered by short, intense rainfall after dry periods. In contrast, longer accumulation periods such as SPEI-12 better represent catchment-scale moisture storage and groundwater contribution, which may be more relevant for N export patterns that depend on longer-term soil water saturation and subsurface flow connectivity.

On the contrary higher annual loads captured by the 90% high-flow threshold in I28 (Appendix 5: Table A2) compared to the event-based analysis (Table 3) may indicate that nutrient export in this catchment is more strongly associated with sustained high-flow conditions rather than distinct hydrological events alone.

SPEI integrates antecedent climatic conditions that influence runoff generation and hydrological connectivity (Vicente-Serrano et al. 2012). In catchments with slower drainage or stronger soil moisture buffering, longer-term moisture accumulation (e.g. reflected in SPEI-12) becomes more relevant for sustaining runoff generation and nutrient transport. In contrast, in more responsive systems, short-term precipitation and rewetting dynamics (captured by SPEI-1) better explain episodic export events linked to rapid rewetting after drought.

4.4 Event identification and implications for nutrient mitigation

In Sweden mitigation programmes have focused on measures at the field level, timing and planning of manure, decreasing autumn ploughing and catch crops (Kyllmar et al. 2023). The implementation of agri-environmental payments for buffer zones had been identified as the most efficient support scheme for reducing

P leaching in Swedish agriculture (Blombäck et al. 2025). Between 2014 and 2024, buffer zones reduced P export by an average of 1.7 tonnes per year at a cost of 17.6 million SEK per tonne. The transition toward narrower buffer zones in the current Strategic Plan (2023–2027) had led to increased cost-efficiency. However, despite their efficiency, a recent evaluation emphasizes that many buffer zones are not placed optimally within the agricultural landscape to achieve maximum nutrient retention. This is particularly critical when considering the high degree of tile drainage in catchment M42, N34, and I28. As previously discussed, subsurface drainage often "short-circuits" the riparian function, allowing nutrients to bypass the buffer strips entirely (Blombäck et al. 2025).

For N on the other hand, the implementation of agri-environmental payments had been focused on catch crops, intermediate crop and spring tillage where it had been identified as the most efficient (Blombäck et al. 2025). These mitigations were also the most cost-efficient, on average, they reduced N leaching from arable land by 911 tonnes per year at a cost of 163,000 SEK per tonne between 2014 and 2024. As an added bonus these mitigations are also found to reduce P leaching, on average, it reduced P leakage by 2.8 tonnes per year between the years 2014 and 2024 (Blombäck et al. 2025).

The cultivation of catch crops is highly dependent on financial compensation (Noring et al. 2023). The occurrence of buffer strips and spring tillage is also dependent on receiving a compensation but to a lesser extent. To get the farmer to apply for a compensation and do the measure it had to be economically beneficial and that the farm had the right conditions for the mitigation e.g., soil type or climate. If the compensations are tied to a five year contract it was even less desired (Noring et al. 2023).

The long-term data for I28, N34, and M42 reveals a significant decline in the cultivation of cover crops starting around 2005 (Linefur et al. 2024). This trend is not an isolated local phenomenon but a direct consequence of the 2005 Common Agricultural Policy (CAP) reform (Emmerman & Karlsson 2010). This reform introduced a paradigm shift in European agriculture through the decoupling of subsidies from production, replacing them with the Single Farm Payment (Gårdsstöd). 70% of the questioned farmers said that in part or whole that the reason for them to have stopped growing catch crops is because of the low compensation (Emmerman & Karlsson 2010). Beside lower compensation the reform introduced cross-compliance, which mandated certain environmental standards as a baseline requirement for receiving any subsidies.

The reduction of cover crops meant that the ability of vegetation to take up residual N during the autumn was significantly weakened. This likely exacerbated the N

leaching peaks observed in M42 and N34 (Figure 8). This suggests that the catchments became more vulnerable to climate variability and extreme weather events since the policy-driven incentives for maintaining continuous soil cover were diminished.

Although mitigation measures contributed to the long-term decline in TN loads observed until approximately 2010, the results suggest that hydroclimatic variability increasingly controls interannual nutrient export and enhanced hydrological connectivity may override the effects of mitigation measures and generate disproportionately high nutrient losses.

Extreme event responses have a substantial impact on the annual loads of TN and TP for years like 1998/1999 in N34 or 1994/1995 in I28. The crops will probably already be saturated during these extreme events, resulting in mitigations such as catch crops, ley, buffer strips may be insufficient when there are high levels of saturation in the soil. Therefore, field-scale measures alone may be insufficient under extreme hydrological conditions, highlighting the need for landscape-scale retention strategies. Increasing the retention with e.g. buffer zones in-stream water storage, ponds or wetlands could be part of the solution. Future mitigation strategies should be designed for the extremes, not for the average conditions. Evaluating best management practices (BMPs) for future climate is therefore key.

Recent studies indicate that combined mitigation strategies may be necessary to achieve substantial reductions in nutrient losses under future climate scenarios. Cover crops in combination with in-stream mitigation have been shown to reduce inorganic N loads by approximately 50% under projected climate conditions, when modelled (Wynants et al. 2024). While additional measures such as reuse of drainage water for irrigation may contribute to nutrient retention at the field scale, their effectiveness depends strongly on economic feasibility and local implementation conditions. At the landscape scale, further reductions in N and P losses may be achieved through structural changes in agricultural systems, including reduced livestock density, increased proportion of leys in crop rotations, and improved redistribution of manure from livestock-intensive to crop-dominated farms (Kyllmar et al. 2023).

4.5 Climate change implications

Since extreme weather events with floods and droughts have become more likely and/or more severe due to climate change (FAO 2025), it will enhance the role of episodic hydrological processes in controlling nutrient export from agricultural catchments. Observed relationships between hydrological conditions and nutrient export suggest that weather variability plays a key role in controlling both TN and

TP losses, particularly during extreme weather years. Under projected climate change, northern Sweden is expected to experience conditions more similar to current southern Swedish climate, including shorter snow-covered periods, reduced soil frost depth, and more frequent freeze–thaw cycles (Norberg et al. 2025). These changes are likely to increase hydrological connectivity and enhance nutrient leaching from agricultural soils. This implies that the patterns of event-driven nutrient export observed in the studied southern catchments may become increasingly relevant further north in the future. In particular, intensified runoff events combined with reduced winter soil protection may lead to higher mobilisation of both TN and TP, especially in systems with tile drainage and high soil content.

4.6 Methodological strengths, limitations and uncertainties

It is important to have long-term monitoring since short-term datasets (<4 years) often fail to capture the high inter-annual variability in nutrient export driven by hydrological fluctuations. This is particularly relevant for P, where event-driven transport can cause large year-to-year variability in total loads (Sharpley et al. 1999). A central problem regarding long-term data sets is in the bridge between different measuring strategies. In this study, this occurred in 2004/2005 for N34 and M42 and in 2005/2006 for I28, when the sampling strategy changed from grab sampling to flow-proportional sampling. Low-frequency monitoring tends to underrepresent episodic events, suggesting that measurements prior to 2005/2006 likely underestimated nutrient transport during hydrological extremes. This is particularly important when evaluating effects of mitigation strategies and analysing trends under a changing climate. The observed shift in TP dynamics in catchment I28 (Figure 11) around 2006–2009 coincides with the transition from manual grab sampling to flow-proportional automated sampling, as well as a change in laboratory analytical methods in 2009. This suggests that the increased variability and higher peak concentrations in the later part of the time series reflect improved monitoring precision rather than a purely biophysical change in the catchment.

4.6.1 Limitations

Predicting nutrient mobilisation in agricultural landscapes is inherently complex, primarily due to significant spatial and temporal variability. Research across diverse catchment characteristics indicates that changes in pollutant loading generally correlate with projected shifts in precipitation and runoff (Coffey et al., 2019). In particular, the increasing frequency of heavy precipitation events is expected to drive more episodic pollutant loading to water bodies, where nutrients accumulated during dry periods are rapidly mobilised during high-flow events

(Coffey et al. 2019; IPCC 2023). All these factors suggest that it is difficult to extrapolate results from one study to another.

Long-term monitoring data of small headwaters under different land uses, climates and land covers, are valuable and essential for assessing the combined effects on water quality and retention in the catchment (De Wit et al. 2020). Few long-term monitoring studies exist that distinguish the significance of water discharge and climatic drivers in relation to nutrient loads (Ezzati et al. 2023).

4.6.2 Uncertainties

First, changes in sampling methodology over time may have influenced the comparability of the data. The introduction of flow-proportional sampling likely resulted in higher and more variable measured concentrations, particularly for P, as peak events are better captured compared to earlier, less frequent sampling approaches (Kyllmar 2009). As shown in Appendix 6: Table A3, manual sampling often underestimated transport during high-flow months (e.g., +94% difference in February 2007 and +87% in March 2009). This suggests that earlier monitoring likely underestimated episodic high-flow transport compared to the later flow-proportional sampling period. Flow-proportional sampling provides a flow-weighted average concentration over the sampling period and is therefore well suited for estimating total nutrient loads. However, short-lived concentration peaks occurring during individual storm events may become diluted. In contrast, grab samples represent instantaneous conditions and may either miss extreme concentrations entirely or, if sampled during an event peak, capture concentrations substantially higher than those represented by flow-proportional samples. In addition, the transition to the SS-EN ISO 6878:2005 analytical method in 2009 may have further enhanced the detection of PP, contributing to the higher TP variability observed in the later part of the time series.

Secondly, the study relies on interpolated values both regarding the weather dataset and the concentrations of TN and TP. The weather dataset includes measurements from different monitoring stations and, in some cases, relies on interpolated values. While efforts were made to ensure consistency, these factors introduce uncertainty. However, the differences between the values used in this study were relatively small, suggesting that the overall impact on the results is limited. The interpolation regarding the nutrients on the other hand is a major limitation in the study.

Nutrient concentrations were originally measured approximately twice per month and subsequently interpolated to a daily time series to match the temporal resolution of discharge data and enable daily load calculations. While this approach allows for continuous load estimation, it introduces uncertainty in the representation of short-term variability, particularly during hydrological extremes. Previous studies have

demonstrated that low-frequency sampling may underestimate short-term nutrient peaks during storm events, particularly for TP, due to the highly episodic nature of transport processes (Bieroza et al. 2014; Lannergård et al. 2021).

As a result, interpolated concentrations tend to smooth temporal variability and may underestimate peak concentrations during event-driven transport, while potentially overestimating concentrations during low-flow periods. Consequently, although daily load estimates provide a useful continuous framework for comparing catchments and hydrological conditions, they should be interpreted with caution.

4.7 Recommendations and future work

Future studies could benefit from combining flow-proportional sampling with high-frequency sensor measurements during extreme runoff events. Such approaches may improve the characterization of short-term nutrient concentration peaks, particularly for PP, and further reduce uncertainties in load estimates. Expanding the use of such methods could help to understand event-driven nutrient losses and their relation to land management practices.

Future studies could also integrate the analysis of SS with TP data to determine the extent to which P transport in these specific catchments is erosion driven. This would clarify whether TP export is primarily particulate-bound or if dissolved subsurface pathways are more dominant in these loam and sandy loam soils.

In addition, a valuable direction for future research would be to analyse whether the frequency of extreme events, defined as SPEI-12 ≤ -1.5 or ≥ 1.5 has increased over the study's period. Such an analysis would provide a more robust understanding of how climate change is directly influencing flow dynamics and the subsequent transport of TN and TP in agricultural catchments.

The results of this study, showing distinct differences in nutrient export between wet years, dry years, and transition periods from dry to wet conditions, indicate that nutrient mobilisation is highly sensitive to hydrological variability. This suggests that under increasingly variable hydrological regimes, current mitigation strategies may need to be re-evaluated to ensure their effectiveness under future climate conditions. This is particularly relevant in the context of hydrological non-stationarity, where changing climate conditions alter the statistical properties of precipitation, runoff, and drought frequency. As a result, historical hydrological records may become less representative of future conditions, reducing the reliability of long-term planning based on past trends alone. This increases the importance of

continuous monitoring and adaptive management approaches in agricultural catchments.

Finally, this study demonstrates that nutrient export is strongly governed by interactions between event-scale hydrology and antecedent climatic conditions, and that both must be considered when evaluating mitigation strategies under changing climatic conditions.

5. Conclusions

Based on the analysis of the three agricultural catchments over three decades, the following conclusions can be drawn to answer the main research question:
How do extreme wet and extreme dry periods affect TN and TP loads in agricultural catchments in southern Sweden?

Wet agrohydrological years were associated with a higher frequency of high-flow events and substantially greater TN and TP export, particularly in catchments N34 and I28. Periods characterised by strongly positive SPEI values contributed disproportionately to annual nutrient loads, highlighting the importance of prolonged wet conditions and hydrological connectivity for nutrient transport.

The results further showed contrasting mobilisation patterns between TN and TP. TN export was primarily associated with sustained hydrological transport and subsurface flow pathways during wet conditions, whereas TP export was more episodic and strongly linked to high-flow events and first-flush responses following drought. These findings suggest that TP may be particularly sensitive to future increases in hydroclimatic variability.

The study also demonstrated that SPEI added important hydrological context beyond runoff-based event identification alone. In particular, SPEI improved the understanding of antecedent moisture conditions, delayed runoff activation and drought-rewetting transitions that influenced nutrient mobilisation processes.

The findings suggest that future mitigation strategies may need to increasingly focus on managing extreme hydrological conditions rather than average conditions alone. As climate change is expected to increase the frequency of extreme weather, future strategies must increasingly shift from the field scale to the landscape scale. Enhanced water retention in the landscape, through constructed wetlands and in-stream water storage, will be crucial to counteract nutrient leaching in a future, more extreme climate.

More broadly, the results highlight the growing importance of understanding how climate variability interacts with agricultural systems and water quality. As hydrological extremes become more frequent in many regions, managing nutrient losses will increasingly require approaches that account not only for average conditions, but also for the extreme events that may dominate ecosystem responses and shape the future resilience of agricultural landscapes.

6. Acknowledgements

I would like to start by thanking the Environmental Monitoring Programme for providing the data that made this project possible. I am especially thankful for Sara Sandström, who stepped in as my supervisor during a critical time and provided valuable guidance and support throughout the whole process. I would also like to thank my assistant supervisor Jennie Barron for helping me see the broader perspective and for her insightful feedback.

References

Allen, R.G. (1998). *Crop evapotranspiration: guidelines for computing crop water requirements*. Food and Agriculture Organization of the United Nations (ed.) (Food and Agriculture Organization of the United Nations, ed.). Food and Agriculture Organization of the United Nations. (FAO irrigation and drainage paper; 56)

Arheimer, B., Andréasson, J., Fogelberg, S., Johnsson, H., Pers, C.B. & Persson, K. (2005). Climate Change Impact on Water Quality: Model Results from Southern Sweden. *AMBIO: A Journal of the Human Environment*, 34 (7), 559–566. https://doi.org/10.1579/0044-7447-34.7.559

Beguería, S. & Vicente-Serrano, S.M. (2023). *SPEI: Calculation of the Standardized Precipitation-Evapotranspiration Index* (1.8.1). https://cran.r-project.org/web/packages/SPEI/index.html [2026-02-17]

Beguería, S., Vicente-Serrano, S.M. & Angulo-Martínez, M. (2010). A Multiscalar Global Drought Dataset: The SPEIbase: A New Gridded Product for the Analysis of Drought Variability and Impacts. *Bulletin of the American Meteorological Society*, 91 (10), 1351–1356. https://doi.org/10.1175/2010BAMS2988.1

Bieroza, M., Heathwaite, A.L., Mullinger, N.J. & Keenan, P.O. (2014). Understanding nutrient biogeochemistry in agricultural catchments: the challenge of appropriate monitoring frequencies. *Environ. Sci.: Processes Impacts*, 16 (7), 1676–1691. https://doi.org/10.1039/C4EM00100A

Bieroza, M.Z. & Heathwaite, A.L. (2015). Seasonal variation in phosphorus concentration–discharge hysteresis inferred from high-frequency *in situ* monitoring. *Journal of Hydrology*, 524, 333–347. https://doi.org/10.1016/j.jhydrol.2015.02.036

Blombäck, K., Beroza, M., Fölster, J., Geranmayeh, P., Johansson, H., Kyllmar, K., Lindsjö, A., Mårtensson, K., Persson, K. & Wesström, I. (2025). *Vattenkvalitet och förluster av kväve och fosfor från jordbruksmark - en utvärdering av stöd och ersättningar i den gemensamma jordbrukspolitiken under åren 2014-2024*. (Utvärderingsrapport 2025:14.). Jordbruksverket.

von Brömssen, C., Betnér, S., Fölster, J. & Eklöf, K. (2020). *Visualizing trends in large-scale environmental data* (v1.0.1). Zenodo. https://doi.org/10.5281/ZENODO.4051247

Canedo Rosso, C., Nyberg, L. & Pechlivanidis, I. (2025). Drought hazard assessment across Sweden's diverse hydro-climatic regimes. *Natural Hazards and Earth System Sciences*, 25 (11), 4577–4592. https://doi.org/10.5194/nhess-25-4577-2025

Chen, S., Zheng, R., Huang, J. & Jiang, S. (2026). High-frequency monitoring reveals rainfall-driven phosphorus and nitrogen concentration–discharge patterns and associated mechanisms. *Journal of Hydrology*, 669, 135151. https://doi.org/10.1016/j.jhydrol.2026.135151

Coffey, R., Paul, M.J., Stamp, J., Hamilton, A. & Johnson, T. (2019). A Review of Water Quality Responses to Air Temperature and Precipitation Changes 2: Nutrients, Algal Blooms, Sediment, Pathogens. *JAWRA Journal of the American Water Resources Association*, 55 (4), 844–868. https://doi.org/10.1111/1752-1688.12711

Crausbay, S.D., Ramirez, A.R., Carter, S.L., Cross, M.S., Hall, K.R., Bathke, D.J., Betancourt, J.L., Colt, S., Cravens, A.E., Dalton, M.S., Dunham, J.B., Hay, L.E., Hayes, M.J., McEvoy, J., McNutt, C.A., Moritz, M.A., Nislow, K.H., Raheem, N. & Sanford, T. (2017). Defining Ecological Drought for the Twenty-First Century. *Bulletin of the American Meteorological Society*, 98 (12), 2543–2550. https://doi.org/10.1175/BAMS-D-16-0292.1

De Wit, H.A., Lepistö, A., Marttila, H., Wenng, H., Bechmann, M., Blicher-Mathiesen, G., Eklöf, K., N. Futter, M., Kortelainen, P., Kronvang, B., Kyllmar, K. & Rakovic, J. (2020). Land-use dominates climate controls on nitrogen and phosphorus export from managed and natural Nordic headwater catchments. *Hydrological Processes*, 34 (25), 4831–4850. https://doi.org/10.1002/hyp.13939

Decker, L., Sawyer, A.H., Welch, S.A., Zhu, J., Binley, A., Field, H.R., Hanrahan, B.R. & King, K.W. (2024). Wide-ranging timescales of subsurface phosphorus transport from field to stream in a tile drained landscape. *Journal of Hydrology*, 635, 131185. https://doi.org/10.1016/j.jhydrol.2024.131185

Dialameh, B. & Ghane, E. (2023). Investigation of phosphorus transport dynamics using high-frequency monitoring at a subsurface-drained field in the Western Lake Erie Basin. *Journal of Great Lakes Research*, 49 (4), 778–789. https://doi.org/10.1016/j.jglr.2023.04.005

Djodjic, F., Börling, K. & Bergström, L. (2004). Phosphorus Leaching in Relation to Soil Type and Soil Phosphorus Content. *Journal of Environmental Quality*, 33 (2), 678–684. https://doi.org/10.2134/jeq2004.6780

van Doorn, M., van Rotterdam, D., Ros, G., Koopmans, G.F., Smolders, E. & de Vries, W. (2024). The phosphorus saturation degree as a universal agronomic and environmental soil P test. *Critical Reviews in Environmental Science and Technology*, 54 (5), 385–404. https://doi.org/10.1080/10643389.2023.2240211

Dupas, R., Faucheux, M., Senga Kiessé, T., Casanova, A., Brekenfeld, N. & Fovet, O. (2024). High-intensity rainfall following drought triggers extreme nutrient concentrations in a small agricultural catchment. *Water Research*, 264, 122108. https://doi.org/10.1016/j.watres.2024.122108

EEA (2025). *Europe's environment 2025*. Publications Office. https://data.europa.eu/doi/10.2800/1121467 [2026-03-10]

Emmerman, A. & Karlsson, A.-M. (2010). *Miljöersättningen odling av fånggröda*. (Miljöersättningen odling av fånggröda, RA10:28). Jordbruksverket.

Eriksson, J. (2011). *Marklära*. Studentlitteratur.

European Commission. Directorate General for Environment., IEEP., Aarhus University., Trinomics., CE Delft., Eunomia., & Cambridge Econometrics. (2021). *Green taxation and other economic instruments: internalising environmental costs to make the polluter pay.* Publications Office. https://data.europa.eu/doi/10.2779/326501 [2026-03-10]

European Parliament and Council (2000). *Directive 2000/60/EC of the European Parliament and of the Council of 23 October 2000 establishing a framework for Community action in the field of water policy*. *Directive 2000/60/EC*. http://data.europa.eu/eli/dir/2000/60/oj [2026-05-12]

Ezzati, G., Kyllmar, K. & Barron, J. (2023). Long-term water quality monitoring in agricultural catchments in Sweden: Impact of climatic drivers on diffuse nutrient loads. *Science of The Total Environment*, 864, 160978. https://doi.org/10.1016/j.scitotenv.2022.160978

FAO (2025). *The State of the World's Land and Water Resources for Food and Agriculture 2025 – The potential to produce more and better*. (2025). https://doi.org/10.4060/cd7488en

Gu, S., Gruau, G., Malique, F., Dupas, R., Petitjean, P. & Gascuel-Odoux, C. (2018). Drying/rewetting cycles stimulate release of colloidal-bound phosphorus in riparian soils. *Geoderma*, 321, 32–41. https://doi.org/10.1016/j.geoderma.2018.01.015

Han, J., Destouni, G., Jarsjö, J., Zhang, Q., Cantoni, J. & Zhang, C. (2024). Legacy sources determine current water quality: Nitrogen and phosphorus in streams of Australia, China, Sweden and USA. *Science of The Total Environment*, 954, 176407. https://doi.org/10.1016/j.scitotenv.2024.176407

Havs- och vattenmyndigheten (2019). *Havs- och vattenmyndighetens föreskrifter om klassificering och miljökvalitetsnormer avseende ytvatten [Swedish Agency for Marine and Water Management's regulations on classification and environmental quality standards regarding surface water]*. (HVMFS 2019:25). https://www.havochvatten.se/download/18.4705beb516f0bcf57ce1c145/1576576601249/HVMFS%202019-25-ev.pdf [2026-05-12]

Intergovernmental Panel On Climate Change (IPCC) (2023). *Climate Change 2022 – Impacts, Adaptation and Vulnerability: Working Group II Contribution to the Sixth Assessment Report of the Intergovernmental*

Panel on Climate Change. 1. ed Cambridge University Press. https://doi.org/10.1017/9781009325844

Jiang, R., Woli, K.P., Kuramochi, K., Hayakawa, A., Shimizu, M. & Hatano, R. (2010). Hydrological process controls on nitrogen export during storm events in an agricultural watershed. *Soil Science and Plant Nutrition*, 56 (1), 72–85. https://doi.org/10.1111/j.1747-0765.2010.00456.x

Johnston, A.E., Poulton, P.R., Fixen, P.E. & Curtin, D. (2014). Phosphorus. In: *Advances in Agronomy*. Elsevier. 177–228. https://doi.org/10.1016/B978-0-12-420225-2.00005-4

de Jonge, L.W., Moldrup, P., Rubæk, G.H., Schelde, K. & Djurhuus, J. (2004). Particle Leaching and Particle-Facilitated Transport of Phosphorus at Field Scale. *Vadose Zone Journal*, 3 (2), 462–470. https://doi.org/10.2136/vzj2004.0462

Jordbruksverket (2023). Bevattning och dränering i jordbruket. https://statistik.jordbruksverket.se/PXWeb/pxweb/sv/Jordbruksverkets%20statistikdatabas/Jordbruksverkets%20statistikdatabas__Arealer__Bevattning%20och%20dranering/JO0112D01.px/table/tableViewLayout2/?loadedQueryId=1916839d-c765-4da9-ba9a-c23c57e3d510&timeType=item [2026-04-24]

Kleinman, P.J.A., Srinivasan, M.S., Dell, C.J., Schmidt, J.P., Sharpley, A.N. & Bryant, R.B. (2006). Role of Rainfall Intensity and Hydrology in Nutrient Transport via Surface Runoff. *Journal of Environmental Quality*, 35 (4), 1248–1259. https://doi.org/10.2134/jeq2006.0015

Kyllmar, K. (2009). *Transporter av kväve och fosfor i vattendrag - inverkan av metodik vid vattenprovtagning*. (Teknisk rapport 131). SLU.

Kyllmar, K., Bechmann, M., Blicher-Mathiesen, G., Fischer, F.K., Fölster, J., Iital, A., Lagzdiņš, A., Povilaitis, A. & Rankinen, K. (2023). Nitrogen and phosphorus losses in Nordic and Baltic agricultural monitoring catchments – Spatial and temporal variations in relation to natural conditions and mitigation programmes. *CATENA*, 230, 107205. https://doi.org/10.1016/j.catena.2023.107205

Kyllmar, K., Forsberg, L.S., Andersson, S. & Mårtensson, K. (2014). Small agricultural monitoring catchments in Sweden representing environmental impact. *Agriculture, Ecosystems & Environment*, 198, 25–35. https://doi.org/10.1016/j.agee.2014.05.016

Lannergård, E.E. (2021). *Phosphorus transport in the landscape: integrating high-frequency monitoring, phosphorus geochemistry and modelling to improve water management*. Swedish University of Agricultural Sciences.

Lannergård, E.E., Fölster, J. & Futter, M.N. (2021). Turbidity-discharge hysteresis in a meso-scale catchment: The importance of intermediate scale events. *Hydrological Processes*, 35 (12), e14435. https://doi.org/10.1002/hyp.14435

Lantmäteriet (2026). Topographic map. https://www.lantmateriet.se/ [2026-03-17]
Lantmet (2026). Agrometeorological Data Service. https://www.slu.se/en/collaborative-centres-and-projects/lantmet/
Linefur, H., Norberg, L., Kyllmar, K., Mårtensson, K. & Blomberg, M. (2024). *Rapportering av Typområden på jordbruksmark*
Liu, Y., Engel, B.A., Flanagan, D.C., Gitau, M.W., McMillan, S.K. & Chaubey, I. (2017). A review on effectiveness of best management practices in improving hydrology and water quality: Needs and opportunities. *Science of The Total Environment*, 601–602, 580–593. https://doi.org/10.1016/j.scitotenv.2017.05.212
Macrae, M., English, M., Schiff, S. & Stone, M. (2009). Influence of Antecedent Hydrologic Conditions on Nitrate and Phosphorus Export from a Small Agricultural Catchment in Southern Ontario, Canada.
Metaxoglou, K. & Smith, A. (2025). Agriculture's nitrogen legacy. *Journal of Environmental Economics and Management*, 130, 103132. https://doi.org/10.1016/j.jeem.2025.103132
Miller, S.A. & Lyon, S.W. (2021). Tile Drainage Increases Total Runoff and Phosphorus Export During Wet Years in the Western Lake Erie Basin. *Frontiers in Water*, 3. https://doi.org/10.3389/frwa.2021.757106
Molina-Navarro, E., Andersen, H.E., Nielsen, A., Thodsen, H. & Trolle, D. (2018). Quantifying the combined effects of land use and climate changes on stream flow and nutrient loads: A modelling approach in the Odense Fjord catchment (Denmark). *Science of The Total Environment*, 621, 253–264. https://doi.org/10.1016/j.scitotenv.2017.11.251
Mosley, L.M. (2015). Drought impacts on the water quality of freshwater systems; review and integration. *Earth-Science Reviews*, 140, 203–214. https://doi.org/10.1016/j.earscirev.2014.11.010
Muhammad, A., Wafae, B., Claudine, D., Alejandro, D.L., Subimal, G., Iskhaq, I., James, K., Sophie, L., Friederike, O., Izidine, P., Masaki, S., M., V.-S., Sergio, Michael, W. & Bolao, Z. (2023). Weather and Climate Extreme Events in a Changing Climate. In: Panmao, Z., Valérie, M.-D., Anna, P., & L., C., Sarah (eds) *Climate Change 2021: The Physical Science Basis. Contribution of Working Group I to the Sixth Assessment Report of the Intergovernmental Panel on Climate Change*. 1. ed. IPCC. 1513–1766. https://doi.org/10.1017/9781009157896
Nilsson, J.E., Weisner, S.E.B. & Liess, A. (2023). Wetland nitrogen removal from agricultural runoff in a changing climate. *Science of The Total Environment*, 892, 164336. https://doi.org/10.1016/j.scitotenv.2023.164336
Norberg, L. (2025). *Catchment N34*[Photograph].
Noring, M., Jörnling, A., Dahlöf, C.-A., Zehaie, F., Klintäng, A.H. & Kätterer, T. (2023). *Effekten på kolinlagring i åkermark*. (Effekten på kolinlagring i

åkermark. Utvärdering av stöd i landsbygdsprogrammet 2014–2022., 2023:9). Jordbruksverket.

Ockenden, M.C., Hollaway, M.J., Beven, K.J., Collins, A.L., Evans, R., Falloon, P.D., Forber, K.J., Hiscock, K.M., Kahana, R., Macleod, C.J.A., Tych, W., Villamizar, M.L., Wearing, C., Withers, P.J.A., Zhou, J.G., Barker, P.A., Burke, S., Freer, J.E., Johnes, P.J., Snell, M.A., Surridge, B.W.J. & Haygarth, P.M. (2017). Major agricultural changes required to mitigate phosphorus losses under climate change. *Nature Communications*, 8 (1), 161. https://doi.org/10.1038/s41467-017-00232-0

Patrick, W.H. & Jugsujinda, A. (1992). Sequential Reduction and Oxidation of Inorganic Nitrogen, Manganese, and Iron in Flooded Soil. *Soil Science Society of America Journal*, 56 (4), 1071–1073. https://doi.org/10.2136/sssaj1992.03615995005600040011x

Peel, M.C., Finlayson, B.L. & McMahon, T.A. (2007). Updated world map of the Köppen-Geiger climate classification. *Hydrology and Earth System Sciences*, 11 (5), 1633–1644. https://doi.org/10.5194/hess-11-1633-2007

Petersen, R.J., Blicher-Mathiesen, G., Rolighed, J., Andersen, H.E. & Kronvang, B. (2021). Three decades of regulation of agricultural nitrogen losses: Experiences from the Danish Agricultural Monitoring Program. *Science of The Total Environment*, 787, 147619. https://doi.org/10.1016/j.scitotenv.2021.147619

R Core Team (2024). *R: A Language and Environment for Statistical Computing* (4.4.2). R Foundation for Statistical Computing. https://www.r-project.org/ [2026-02-17]

Samsonov, T. (2025). *grwat: River Hydrograph Separation and Analysis* (0.1). https://cran.r-project.org/package=grwat

Sandström, S., Futter, M.N., Kyllmar, K., Bishop, K., O'Connell, D.W. & Djodjic, F. (2020). Particulate phosphorus and suspended solids losses from small agricultural catchments: Links to stream and catchment characteristics. *Science of The Total Environment*, 711, 134616. https://doi.org/10.1016/j.scitotenv.2019.134616

Sharpley, A.N., Daniel, T., Sims, T., Lemunyon, J., Stevens, R. & Parr, R. (1999). *Agricultural Phosphorus and Eutrophication*. https://doi.org/10.22004/AG.ECON.373388

Sharpley, A.N., Kleinman, P.J.A., McDowell, R.W., Gitau, M. & Bryant, R.B. (2002). Modeling phosphorus transport in agricultural watersheds: Processes and possibilities. *Journal of Soil and Water Conservation*, 57 (6), 425–439. https://doi.org/10.1080/00224561.2002.12457475

Sjulgård, H., Keller, T., Garland, G. & Colombi, T. (2023). Relationships between weather and yield anomalies vary with crop type and latitude in Sweden. *Agricultural Systems*, 211, 103757. https://doi.org/10.1016/j.agsy.2023.103757

SLU (2025). *Monitoring of agricultural catchments*. https://www.slu.se/en/environment/statistics-and-environmental-data/environmental-data-catalogue/monitoring-of-agricultural-catchments/ [2026-04-24]

SMHI (2026). Meteorological Observations and Records. https://www.smhi.se/data [2026-02-28]

Sobota, D.J., Compton, J.E., McCrackin, M.L. & Singh, S. (2015). Cost of reactive nitrogen release from human activities to the environment in the United States. *Environmental Research Letters*, 10 (2), 025006. https://doi.org/10.1088/1748-9326/10/2/025006

Statistiska centralbyrån (2024). *Nitrogen and phosphorus balances for agricultural land in 2022*. SCB.

Svensson, J. (2022). Bedömningsgrunder för ytvattenförekomster.

Swedish University of Agricultural Sciences (SLU) (2026). National data host lakes and watercourses, and national data host agricultural landView(annual_table). https://miljodata.slu.se/mvm/ [2026-02-07]

Teutschbein, C., Quesada Montano, B., Todorović, A. & Grabs, T. (2022). Streamflow droughts in Sweden: Spatiotemporal patterns emerging from six decades of observations. *Journal of Hydrology: Regional Studies*, 42, 101171. https://doi.org/10.1016/j.ejrh.2022.101171

Van Meter, K.J., Basu, N.B., Veenstra, J.J. & Burras, C.L. (2016). The nitrogen legacy: emerging evidence of nitrogen accumulation in anthropogenic landscapes. *Environmental Research Letters*, 11 (3), 035014. https://doi.org/10.1088/1748-9326/11/3/035014

Vattenmyndigheterna (2025). VISS – Vatteninformationssystem Sverige. https://ext-webbgis.lansstyrelsen.se/e17e00dc-cfac-4314-a619-ec4533254346/ [2026-03-09]

Vicente-Serrano, S.M., Beguería, S. & López-Moreno, J.I. (2010). A Multiscalar Drought Index Sensitive to Global Warming: The Standardized Precipitation Evapotranspiration Index. *Journal of Climate*, 23 (7), 1696–1718

Vicente-Serrano, S.M., Beguería, S., Lorenzo-Lacruz, J., Camarero, J.J., López-Moreno, J.I., Azorin-Molina, C., Revuelto, J., Morán-Tejeda, E. & Sanchez-Lorenzo, A. (2012). Performance of Drought Indices for Ecological, Agricultural, and Hydrological Applications. *Earth Interactions*, 16 (10), 1–27. https://doi.org/10.1175/2012EI000434.1

Weigelhofer, G., Ramião, J.P., Pitzl, B., Bondar-Kunze, E. & O'Keeffe, J. (2018). Decoupled water-sediment interactions restrict the phosphorus buffer mechanism in agricultural streams. *Science of The Total Environment*, 628–629, 44–52. https://doi.org/10.1016/j.scitotenv.2018.02.030

Wilhite, D. & Glantz, M. (1985). Understanding: the Drought Phenomenon: The Role of Definitions. *Water International - WATER INT*, 10, 111–120. https://doi.org/10.1080/02508068508686328

Williams, M.R., King, K.W., Macrae, M.L., Ford, W., Van Esbroeck, C., Brunke, R.I., English, M.C. & Schiff, S.L. (2015). Uncertainty in nutrient loads from tile-drained landscapes: Effect of sampling frequency, calculation algorithm, and compositing strategy. *Journal of Hydrology*, 530, 306–316. https://doi.org/10.1016/j.jhydrol.2015.09.060

World Meteorological Organization & Global Water Partnership (2016). *Handbook of drought indicators and indices*. World Meteorological Organization. https://www.droughtmanagement.info

Wurtsbaugh, W.A., Paerl, H.W. & Dodds, W.K. (2019). Nutrients, eutrophication and harmful algal blooms along the freshwater to marine continuum. *Wiley Interdisciplinary Reviews: Water*, 6 (5). https://doi.org/10.1002/WAT2.1373

Wynants, M., Strömqvist, J., Hallberg, L., Livsey, J., Lindström, G. & Bieroza, M. (2024). How to Achieve a 50% Reduction in Nutrient Losses From Agricultural Catchments Under Different Climate Trajectories? *Earth's Future*, 12 (7), e2023EF004299. https://doi.org/10.1029/2023EF004299

Yang, Y.-Y., Asal, S. & Toor, G.S. (2021). Residential catchments to coastal waters: Forms, fluxes, and mechanisms of phosphorus transport. *Science of The Total Environment*, 765, 142767. https://doi.org/10.1016/j.scitotenv.2020.142767

Popular science summary

Climate change is expected to make extreme weather events such as heavy rainfall and droughts more frequent and intense. In agricultural landscapes, this can strongly influence how nutrients from farmland are transported into nearby streams and rivers, where they may contribute to problems such as algal blooms and oxygen depletion.

This study investigates how long-term weather variability affects nitrogen and phosphorus losses from agricultural catchments in southern Sweden. It is based on 30 years of environmental monitoring data from three small agricultural catchments. By combining water quality measurements with weather data, the study explores how periods of unusually wet or dry conditions influence nutrient transport.

The results show that wet periods are particularly important for nutrient losses. During extended wet conditions, more water moves through the landscape, increasing the transport of both nitrogen and phosphorus into streams. In some cases, a relatively small number of wet days accounted for a large share of the total annual nutrient losses. Nitrogen was mainly transported gradually through the soil via subsurface flow, while phosphorus losses were more episodic and linked to short, intense rainfall events.

The study also highlights the importance of recent weather conditions. Moisture conditions over the past month were strongly linked to how much nutrients were lost from the landscape. While dry periods generally reduced nutrient export, long droughts followed by heavy rainfall could temporarily trigger sharp pulses of nutrient losses.

Overall, the findings suggest that current mitigation measures at field scale may not be sufficient under increasingly extreme weather conditions. Instead, future strategies should focus more on landscape-scale water retention to reduce nutrient transport in a changing climate.

Appendix 1

Description of Penman-Monteith equation

G (Soil Heat Flux): The energy used to heat the soil ($MJ/m^2/day$). Soil heat flux (G) was assumed negligible at the daily scale.

es (Saturation Vapor Pressure): The maximum amount of moisture the air can hold at a given temperature (kPa). To account for the non-linear relationship between temperature and vapor pressure, es is calculated by averaging the saturation vapor pressures at T_{max} and $T_{min.}$

ea (Actual Vapor Pressure): The actual amount of moisture present in the air, derived from the Relative Humidity and the temperature data.

es - ea (Vapor Pressure Deficit, VPD): This represents the "thirst" of the atmosphere; a higher deficit indicates a greater potential for evaporation.

γ = (Psychrometric Constant)

Appendix 2

Classification

Step 1 For catchments, the reference value is calculated according to the following Equation A1:

(A1) $\mathrm{LogTotPref} = 1.393 + 0.574 \times \mathrm{logAbsF} + 0.451 \times \mathrm{logClay} - 0.249 \times \mathrm{logSO4} + 0.264 \times \log(\mathrm{Ca} + \mathrm{Mg}) - 0.0629 \times \mathrm{logTotal} - 0.129 \times \mathrm{logMarsh} + 0.0425 \times \mathrm{logWater}$

where: TotPref is calculated in µg/l

AbsF = the absorbance at 420 nm on filtered sample with 5cm cuvette

Clay = average clay content in the entire catchment area in % + 1. The clay content in the catchment is calculated by area weighting of the clay content in the agricultural land (multiplication by the proportion of agricultural land in the river basin in % by 100).

SO_4 = sulphate content in meq/l Ca+Mg = sum of the calcium and magnesium levels in meq/l

Alt = altitude in m

Marsh soil = proportion of marsh land in the catchment area in % + 1

Water = the proportion of water surface in the catchment area in %

Logarithms refer to the base 10 and to the clay content and the proportion of marshland, the value 1 is added in order to be able to calculate logarithms for all waters even when the proportion is 0.

If data for SO_4 are missing, or if high SO_4 concentrations are suspected to be due to factors other than mud marshes in the catchment area, the alternative Equation A2 is used.

(A2) $\mathrm{LogTotPref} = 1.484 + 0.519 \times \mathrm{logAbsF} + 0.472 \times \mathrm{logClay} - 0.0616 \times \mathrm{logTotal} - 0.0986 \times \mathrm{logMarsh}$

Appendix 3

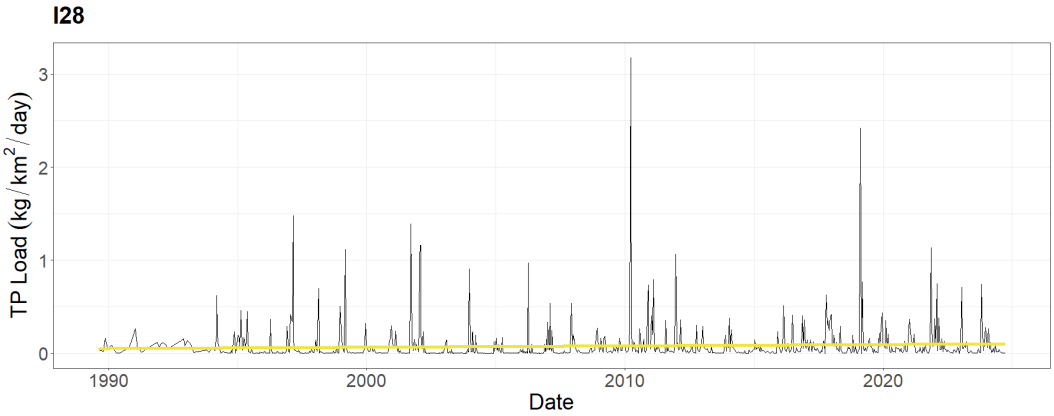

Figure A1. Trend curve for total phosphorus (TP) load (kg/km²/day) in I28 (1989 – 2025) produced by a generalised additive model (GAM). Colour indicates periods with significant trends, decreasing (blue), increasing (red), and no significant trend (yellow), based on the first derivative of the smooth term (95% confidence interval). Observed values are shown as black points/lines, and the smooth curve represents the fitted long-term trend including seasonal variation.

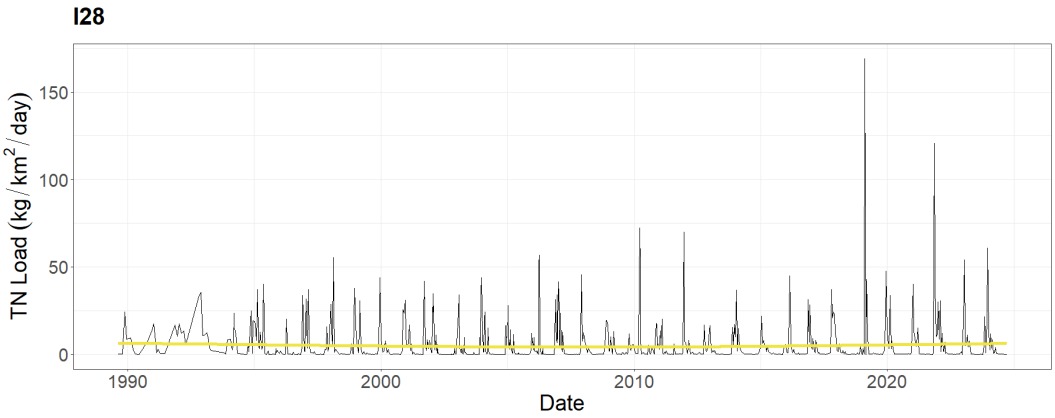

Figure A2. Trend curve for total nitrogen (TN) load (kg/km²/day) in I28 (1989 – 2025) produced by a generalised additive model (GAM). Colour indicates periods with significant trends, decreasing (blue), increasing (red), and no significant trend (yellow), based on the first derivative of the smooth term (95% confidence interval). Observed values are shown as black points/lines, and the smooth curve represents the fitted long-term trend including seasonal variation.

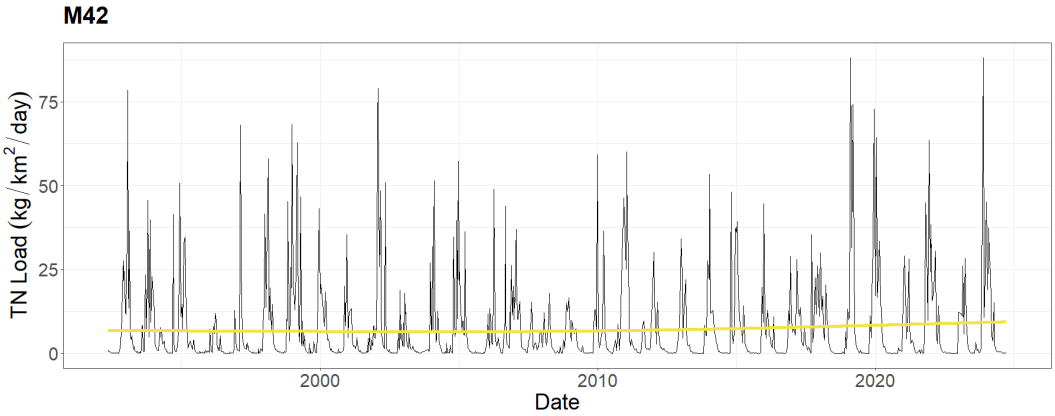

Figure A3. Trend curve for total nitrogen (TN) load (kg/km²/day) in M42 (1993 – 2024) produced by a generalised additive model (GAM). Colour indicates periods with significant trends, decreasing (blue), increasing (red), and no significant trend (yellow), based on the first derivative of the smooth term (95% confidence interval). Observed values are shown as black points/lines, and the smooth curve represents the fitted long-term trend including seasonal variation.

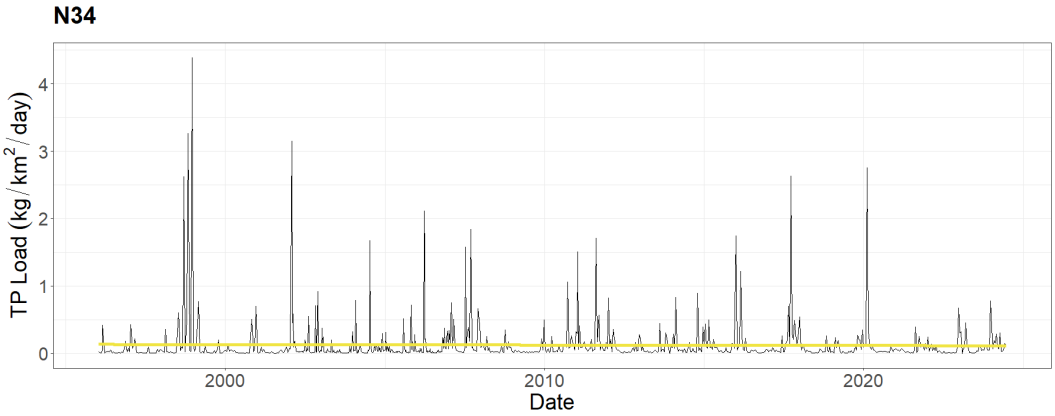

Figure A4. Trend curve for total phosphorus (TP) load (kg/km²/day) in N34 (1996 – 2024) produced by a generalised additive model (GAM). Colour indicates periods with significant trends, decreasing (blue), increasing (red), and no significant trend (yellow), based on the first derivative of the smooth term (95% confidence interval). Observed values are shown as black points/lines, and the smooth curve represents the fitted long-term trend including seasonal variation.

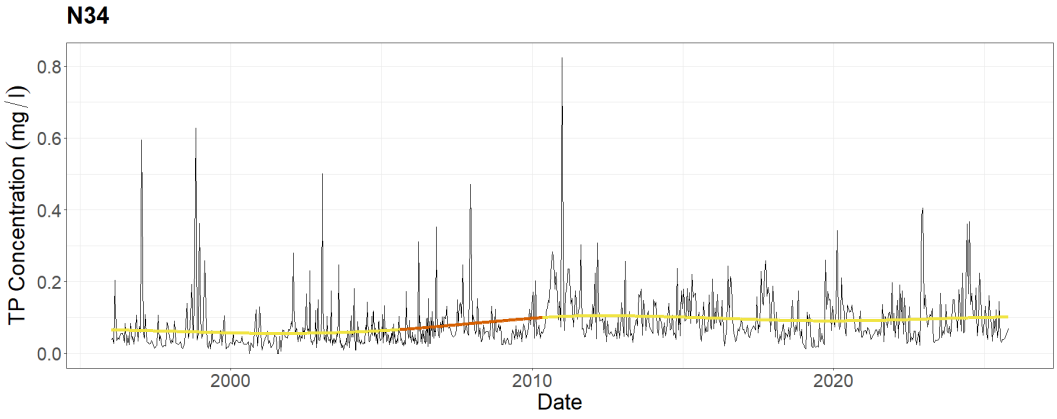

Figure A5. Trend curve for total phosphorus (TP) concentration (mg/l) in N34 (1996 – 2024) produced by a generalised additive model (GAM). Colour indicates periods with significant trends, decreasing (blue), increasing (red), and no significant trend (yellow), based on the first derivative of the smooth term (95% confidence interval). Observed values are shown as black points/lines, and the smooth curve represents the fitted long-term trend including seasonal variation.

Appendix 4

Table A1. Full description of annual total nitrogen (TN) and total phosphorus (TP) loads in I28, M42 and N34 based on monthly transport of nutrients.

	Annual TN Load (kg/km^2)			Annual TP load (kg/km^2)		
Year	I28	M42	N34	I28	M42	N34
1989/1990	1718.2			15.576		
1990/1991	1541.6			22.991		
1991/1992	1747.2			13.231		
1992/1993	2369			16.386		
1993/1994	1117.9			12.372		
1994/1995	2590.6			25.708		
1995/1996	336.9		1051.9	3.565		6.638
1996/1997	1294.3		2732.8	30.204		16.373
1997/1998	2152.3		3673.9	12.515		11.753
1998/1999	1461		6766	25.551		113.044
1999/2000	1621.7		3628.9	15.606		13.733
2000/2001	1723.2		3180.7	19.175		13.931
2001/2002	1417.6		5712.8	36.231		52.916
2002/2003	866.3		3383.6	4.247		28.97
2003/2004	1273.6		2972.4	14.956		21.008
2004/2005	1302.3		4343.2	10.731		35.2975
2005/2006	1145.2		3132	11.3015		29.071
2006/2007	1924.35	3433.1	4576.35	15.6035	65.535	40.48
2007/2008	1208.35	1776.6	3681.3	13.289	42.306	65.64
2008/2009	1821.3	1678.6	2495.9	23.0905	15.509	21.0425
2009/2010	1468.2	1593.3	2266.45	53.861	24.968	22.677
2010/2011	1755.8	3351.4	2764.2	60.402	58.97	65.23
2011/2012	1389.7	1783.2	3407	37.148	42.881	48.401
2012/2013	1169.6	1984.6	2098.7	23.333	35.1	19.203
2013/2014	2014.3	2376.4	3154.1	21.419	37.331	35.183
2014/2015	1380.1	2996.1	3480.5	15.617	61.73	48.959
2015/2016	982.9	2249	3280.8	20.68	45.406	36.721
2016/2017	1620.1	2556.3	1780.8	35.178	31.631	11.283
2017/2018	2454.2	3396.2	5256	73.644	76.355	91.857
2018/2019	2211.1	3491.6	3807.2	47.421	20.192	19.361
2019/2020	2088.4	4517.5	3964.3	39.46	37.328	47.636
2020/2021	1899.4	2188.9	2488	43.573	24.577	15.874
2021/2022	3704.5	4382.8	3125.5	56.477	68.81	31.479
2022/2023	2029.8	2794.1	3146.7	26.418	34.611	31.007
2023/2024	2305.4	4720.3	4073.7	31.177	73.593	56.757
2024/2025	1070.5			8.318		

Appendix 5

Table A2. Number of high-flow events and the proportion of total nitrogen (TN) and phosphorus (TP) export occurring during events in the three catchments (I28, M42 and N34) under wet and dry agrohydrological years. High-flow events were defined as days exceeding the 90th percentile of discharge, with consecutive event days grouped into single events.

Catchment	Agrohydrological year	Characterised	Number of events	TN of annual load (%)	TP of annual load (%)
I28	1994/1995	Wet	12	55	51
I28	1998/1999	Wet	9	62	65
I28	2005/2006	Dry	8	76	83
I28	2015/2016	Dry	9	60	37
M42	1993/1994	Wet	8	43	52
M42	2007/2008	Wet	12	32	38
M42	2019/2020	Dry	7	43	43
M42	2023/2024	Dry	6	46	44
N34	1998/1999	Wet	14	43	59
N34	1999/2000	Wet	15	40	38
N34	2016/2017	Dry	7	34	24
N34	2018/2019	Dry	6	45	53

Appendix 6

Table A3. Top 15 months in catchment I28 with the largest percentage difference between manual grab sampling and flow-proportional automated sampling for total phosphorus (TP) load (kg/km²).

Month	TP Manuell (kg/km²)	TP Flow prop. (kg/km²)	Difference (%)
2006-03	4.529	3.874	-14.5
2007-01	4.684	4.031	-13.9
2007-02	3.385	6.567	+94.0
2007-03	2.502	3.376	+34.9
2007-11	0.750	1.169	+55.9
2007-12	4.715	6.309	+33.8
2008-01	3.164	3.639	+15.0
2008-11	4.371	6.198	+41.8
2009-03	4.318	8.093	+87.4
2009-07	4.714	3.384	-28.2
2009-12	5.429	6.668	+22.8
2010-03	27.331	25.199	-7.8
2010-04	5.346	3.629	-32.1
2010-05	2.294	1.260	-45.1
2010-06	3.995	1.277	-68.0

Appendix 7

Table A4. Historical overview of data ownership, laboratories, and analytical standards (SLU 2026).

Period	Catchment ID	Data Owner	Analytical Laboratory	Method/ISO (TP)	Method/ISO (TN)
1989-1997	I28	County Admin. Board	Lantbrukskem, Visby	SS 028127-2 (mod)	Tec. ASN 110-03/92
1988-2002	M42, N34	County Admin. Board	SLU, Soil and Environment	SS 028127-2	SIS 028131-1
1997-2002	I28	County Admin. Board	ScanCem / Cementa	SS 028127-2	SS 028131-1
2002-2008	All	Swedish EPA[1]	SLU, Soil and Environment	SS-EN 1189-1	SS-EN ISO 11905-1
2009-2014	All	Swedish EPA[1]	SLU, Soil and Environment	SS-EN ISO 6878:2005	SS-EN ISO 11905-1
2014-2021	All	Swedish EPA[1]	SLU, Aquatic Sciences	SS-EN ISO 6878:2005	SS-EN ISO 11905-1
2021-2025	All	Swedish EPA[1]	SLU, Aquatic Sciences	SS-EN ISO 6878:2005	SS-EN ISO 20236:2021

1. Swedish EPA (Naturvårdsverket) assumed national responsibility for the agricultural monitoring program in 2002.

Appendix 8

Table A5. Quantitative analysis of nutrient export during periods of hydrological extremes. The data represents the total area-specific load for each period and the proportion of that load occurring during days when the catchment was under extreme hydrological pressure based on the SPEI-3 index (>1.5 for wet and <-1.5 or <-1.0 for dry conditions).

Catchment ID	Study Period	Characterised	SPEI-3 Threshold	Days in Extreme Zone (%)	Total TN-Load (kg/km^2)	Total TN-load (%)	Total TP-Load (kg/km^2)	Total TP-load (%)
I28	2005/2006	Dry	< -1.0*	78 (21)	1	0.2	12	1.2
I28	2002–2007	Dry period	< -1.0	662 (30)	8	0.2	91	0.9
M42	2023/2024	Dry	< -1.5	36 (10)	5	0.1	78	0.5
M42	2018–2024	Dry period	< -1.5	485 (19)	25	0.2	347	0.8
N34	1998/1999	Wet	> 1.5	168 (46)	7	62	114	82
N34	1998–2002	Wet period	> 1.5	294 (16)	24	31	219	54

**For catchment I28, a threshold of -1.0 was applied as the SPEI-3 index did not fall below -1.5 during the specific agrohydrological year 2005/2006.*

Publishing and archiving

Approved students' theses at SLU can be published online. As a student you own the copyright to your work and in such cases, you need to approve the publication. In connection with your approval of publication, SLU will process your personal data (name) to make the work searchable on the internet. You can revoke your consent at any time by contacting the library.

Even if you choose not to publish the work or if you revoke your approval, the thesis will be archived digitally according to archive legislation.

You will find links to SLU's publication agreement and SLU's processing of personal data and your rights on this page:

- https://libanswers.slu.se/en/faq/228318

☒ YES, I, Inger, have read and agree to the agreement for publication and the personal data processing that takes place in connection with this